AVC-VTN-10-G01
(=SAIC-10/2201)

Exploitation of the IMS and Other Data for a Comprehensive Advanced Analysis of the North Korean Nuclear Tests

J. R. Murphy
B. C. Kohl
J. L. Stevens
T. J. Bennett
H. G. Israelsson

Final Technical Report
Under DOS Contract No. SAQMMA09C0250
(09/01/2009 – 08/31/2010)

Submitted to
U. S. Department of State
2201 C Street, NW
Washington, DC 20520

February 2010

Approved for Public Release; Distribution Unlimited

REPORT DOCUMENTATION PAGE	*Form Approved OMB No. 0704-0188*

PLEASE DO NOT RETURN YOUR FORM TO THE ABOVE ORGANIZATION.

1. REPORT DATE *(DD-MM-YYYY)*	**2. REPORT TYPE**	**3. DATES COVERED** *(From - To)*
18-02-2010	Technical Report	19-09-2009 - 18-02-2010

4. TITLE AND SUBTITLE
Exploitation of the IMS and Other Data for a Comprehensive Advanced Analysis of the North Korean Nuclear Tests

5a. CONTRACT NUMBER
SAQMMA09C0250

5b. GRANT NUMBER

5c. PROGRAM ELEMENT NUMBER

6. AUTHOR(S)
Murphy, J. R., Kohl, B. C., Stevens, J. L., Bennett, T. J., Israelsson, H. G.

5d. PROJECT NUMBER

5e. TASK NUMBER

5f. WORK UNIT NUMBER

7. PERFORMING ORGANIZATION NAME(S) AND ADDRESS(ES)
SAIC
8301 Greensboro Drive
M/S E 5-6
McLean, VA 22102

8. PERFORMING ORGANIZATION REPORT NUMBER
SAIC-10/2201

9. SPONSORING/MONITORING AGENCY NAME(S) AND ADDRESS(ES)
U.S. Department of State / VCI
2201 C Street, N.W.
Washington, DC 20520
Attn: Rongsong Jih (202-647-8126)

10. SPONSOR/MONITOR'S ACRONYM(S)
DOS/VCI/TA

11. SPONSOR/MONITOR'S REPORT NUMBER(S)

12. DISTRIBUTION/AVAILABILITY STATEMENT
Unlimited

13. SUPPLEMENTARY NOTES

14. ABSTRACT
On May 25, 2009 the North Koreans conducted a second underground nuclear test at a location very close to that of their initial 2006 test in a remote, mountainous region of northeastern North Korea. The objective of this study was to exploit International Monitoring System (IMS) and other open data sources to conduct comprehensive, advanced analyses of the characteristics of these two North Korean nuclear tests. These studies focused on refining event locations, estimating source depths and seismic yields and evaluating the effectiveness of the various seismic event identification criteria as applied to these two explosions. Seismic data recorded at stations of the global IMS network were augmented with seismic data from key regional stations (<20 degrees) obtained from the Incorporated Research Institutions for Seismology (IRIS) data management center, the Ocean Hemisphere Project Data Management Center (OP HDMC) and the Japanese National Research Institute for Earth Science and Disaster Prevention (NIED).

15. SUBJECT TERMS
North Korea nuclear explosion seismic

16. SECURITY CLASSIFICATION OF:			**17. LIMITATION OF ABSTRACT**	**18. NUMBER OF PAGES**	**19a. NAME OF RESPONSIBLE PERSON**
a. REPORT	**b. ABSTRACT**	**c. THIS PAGE**			John R. Murphy
Unclassified	Unclassified	Unclassified	UU	51	**19b. TELEPHONE NUMBER** *(Include area code)* 703-676-4366

Standard Form 298 (Rev. 8/98)
Prescribed by ANSI Std. Z39.18
Adobe Professional 7.0

Executive Summary

On May 25, 2009 the North Koreans conducted a second underground nuclear test at a location very close to that of their initial 2006 test in a remote, mountainous region of northeastern North Korea. The objective of the present study has been to exploit IMS and other open data sources to conduct comprehensive, advanced analyses of the characteristics of these two North Korean nuclear tests. These studies focused on refining event locations, estimating source depths and seismic yields and evaluating the effectiveness of the various seismic event identification criteria as applied to these two explosions. Seismic data recorded at stations of the global IMS network were augmented with seismic data from key regional stations (Δ<20degrees) obtained from the Incorporated Research Institutions for Seismology (IRIS) data management center, the Ocean Hemisphere Project Data Management Center (OP HDMC) and the Japanese National Research Institute for Earth Science and Disaster Prevention (NIED). The principal findings of these analyses with regard to the characterization of the North Korean nuclear tests can be summarized as follows:

- Available seismic arrival time data from the 2006 and 2009 tests were analyzed using a variety of state-of-the-art relative location techniques. All of the resulting solutions yielded very similar locations, indicating that the 2009 test was conducted about 2.5 km west-northwest of the 2006 test. Supplemental topographic data for the site were used to further constrain the absolute locations with respect to the tunnel adit entry identified from open source overhead imagery.
- Teleseismic P wave spectral data were inverted using a model-based procedure to determine the yield of the 2009 test. Because source depth is poorly constrained using conventional seismic techniques, yield estimates were determined at 100 m increments over the plausible depth range from 100 to 800 m. These yield estimates vary from 2.0 to 4.8 kt.
- Since the uncertainty in source depth leads to considerable uncertainty in the yield estimate, a new technique based on broadband source spectral ratios was developed to better constrain the depths of the 2006 and 2009 explosions. The results of this analysis indicate that the two explosions could not have been conducted at any common depth in the plausible 100 to 800 m range; and, in fact, the observed spectral ratio data are best modeled by source depths of about 200 m for the 2006 test and 550 m for the 2009 test. The corresponding yield estimates for the 2006 and 2009 tests are 0.9 kt and 4.6 kt., respectively.
- Relative yield estimates based on Lg observations from the two tests are generally consistent with the yield estimates obtained by modeling the network-averaged teleseismic P wave spectra and the estimates obtained by modeling the regional, broadband P wave source spectral ratios.
- The long-period surface wave Ms magnitudes for both the 2006 and 2009 tests appear to be anomalously large relative to historical experience, producing unreasonably large Ms yield estimates and problematic Ms/mb identification characteristics. A formal moment tensor inversion analysis of the available data has indicated that release of tectonic strain energy by the explosion may have contributed somewhat to the observed anomaly. However, current estimates of the likely strength of this tectonic release are not large enough to fully explain the observed anomaly. Additional research will be required to

determine whether unresolved CLVD secondary sources may account for the discrepancy.

- Identification of the 2009 and 2006 events as explosions based on high-frequency Pn/Lg ratios measured at regional stations are unambiguous; however, results for discrimination based on Ms-versus-mb are inconclusive (again probably due to secondary source contamination to Ms).

Table of Contents

1 Introduction

1.1 Event Parameters

The May 25, 2009 underground nuclear test conducted by North Korea (Democratic People's Republic of Korea, DPRK) was located in the same general area of northeastern North Korea where a previous nuclear test was conducted in 2006 (Figure 1). The two events appear to have been conducted in the same tunnel complex mined into Mount Mantap. The area is a relatively stable craton (the North China-Korean platform) with a basement of Archean (~2000 Ma BP) and Proterozoic (~1000 Ma BP) granite and metamorphosed rocks which are overlain by up to 1 km of Cenozoic (65 Ma BP – Present) volcanic basalts which are little deformed (USGS, 1967).

Although rather small in magnitude, the 2009 test was recorded by numerous global seismic stations, including 56 stations of the International Monitoring System (IMS). As shown in Table 1, seismic locations determined by the International Data Centre (IDC), US Geological Survey (USGS/NEIC), and independently in relative location analyses by SAIC (described below) are located in proximity to a tunnel entrance previously identified from satellite imagery analyses and believed to be associated with the 2006 explosion (GlobalSecurity.org, 2006; Schlittenhadt et al., 2010).

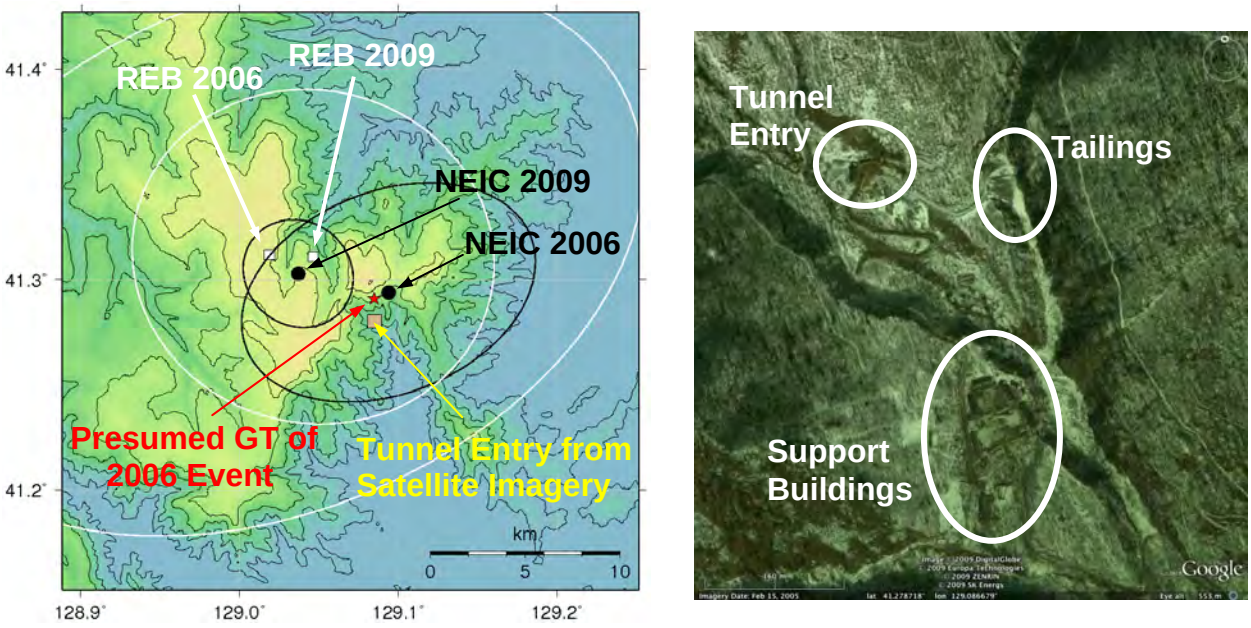

Figure 1. Seismic locations (left) of 2009 and 2006 North Korean nuclear tests relative to tunnel entry (based on satellite imagery) and preferred ground truth (GT) for the 2006 event developed from imagery (right) and topography analysis.

Table 1. Locations of 2006 and 2009 North Korean nuclear tests from various sources.

		Lat (°N)	Lon (°E)	Error Ellipse Area (km^2)	No. Stations Used	No. Stations within 2000 km	Largest Azimuth Gap
Tunnel Entry (satellite)		41.2803	129.0852	NA	NA	NA	NA
2006	IDC REB	41.3119	129.0189	879	22	3	~112°
	USGS/NEIC	41.294	129.094	136	31	8	~73°
	ISC	41.2363	129.0849	76	68	10	~51°
	SAIC (preferred)	41.2867	129.0902	NA (fixed)*	NA	NA	NA
2009	IDC REB	41.3110	129.0464	265	56	6	~53°
	USGS/NEIC	41.303	129.037	26	131	15	~41°
	SAIC	41.2925	129.0657	< 0.2 (relative)*	35-66	8-41	~72°

* Error ellipse estimates for relative location techniques are based on assumed accurate location of the fixed reference event.

An important element in characterizing the 2009 North Korean nuclear test is determination of its source size. Seismic magnitudes for the 2009 and 2006 explosion tests based on a variety of seismic phase measurements, as estimated by IDC and USGS, are shown in Table 2. As described below, some of these magnitude measures may be more robust than others for use in determining the yield (based on magnitude/yield relationships) for the 2009 North Korean test and some appear to be anomalous.

Table 2. Seismic network magnitudes from various phase measurements reported by different authorities.

	2009			2006		
	Magnitude	# Stations	Distance Range	Magnitude	# Stations	Distance Range
IDC – mb	4.5	45	~23-95°	4.1	16	~33-81°
IDC – mb1	4.6	51	~4-95°	4.2	20	~8-81°
IDC – ML	4.3	6	~4-17°	3.9	4	~8-17°
IDC – Ms	3.6	15	~4-77°	NA	NA	NA
USGS – mb	4.7	54	~34-93°	4.3	11	~21-72°
USGS – ML	4.2	2	~4°	4.2	2	~3-4°
USGS – mb(Lg)	3.6	4	~4-19°	3.6	3	~3-9°
SAIC – Ms*	3.66	6	~3-20°	2.93	6	~3-20°

* SAIC used methods comparable to IDC analyses to develop Ms magnitudes at seven regional stations for the 2006 North Korean test.

1.2 Data Resources

The primary and auxiliary seismic networks of the International Monitoring System (IMS) were the principal sources of data for the analysis conducted in this study. Signals from the 2009 test were detected globally on 56 IMS stations (Figure 2) as reported in the Reviewed Event Bulletin of the International Data Centre. Figure 3 shows a sample of the waveforms showing good SNR even at remote stations.

We supplemented the IMS data with key regional stations (< 20 degrees) from three sources:

- Incorporated Research Institutions for Seismology (IRIS) data management center
  - Global Seismograph Network (II and IU networks) – numerous stations at regional and teleseismic distances, in particular INCN (Incheon Korea)
  - New Chinese Digital Seismic Network (IC network) – numerous stations at regional distances, in particular MDJ (Mudanjiang, China) the closest station which recorded both events
  - Kazakhstan Network (KZ) – stations at regional distance
  - Kyrgyz Seismic Telemetry Network (KNET) – stations at regional distance
- Ocean Hemisphere Project Data Management Center (OP HDMC) – included TJN (Teajon, Korea) at a distance of about 500 km
- National Research Institute for Earth Science and Disaster Prevention (NIED) – a network of over 40 stations in Japan, all within regional distance

Emphasis was on obtaining broadband waveform data from stations that recorded signals from both the 2006 and 2009 events. This supported the detailed comparative analysis conducted in much of this report.

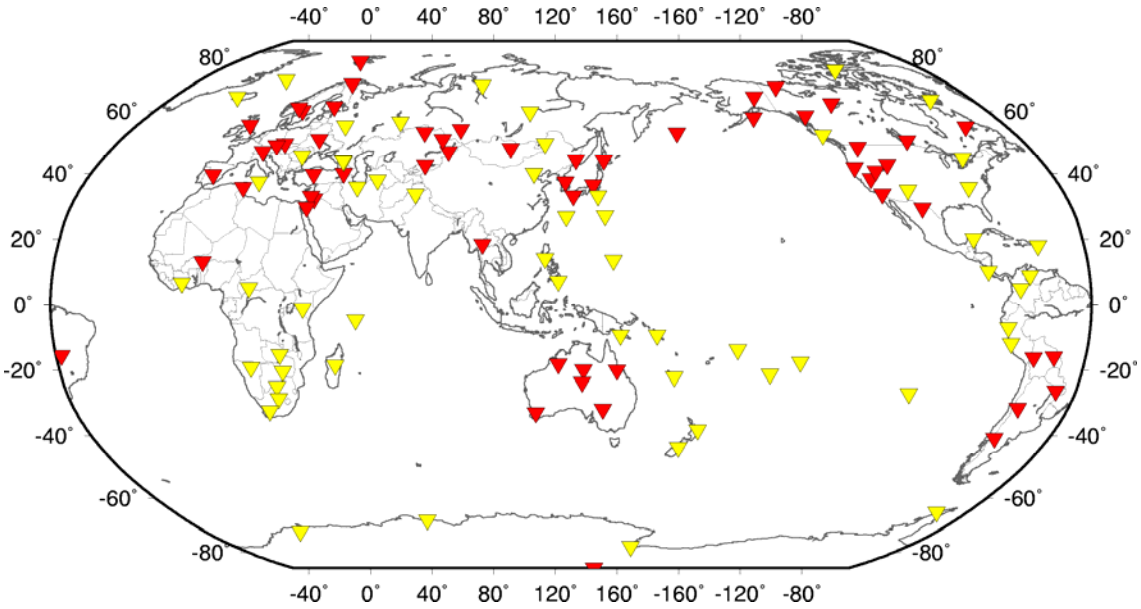

Figure 2. Seismic stations of the IMS primary and auxiliary networks that detected (red) and did not detect (yellow) the May 25, 2009 nuclear test as reported in the IDC REB.

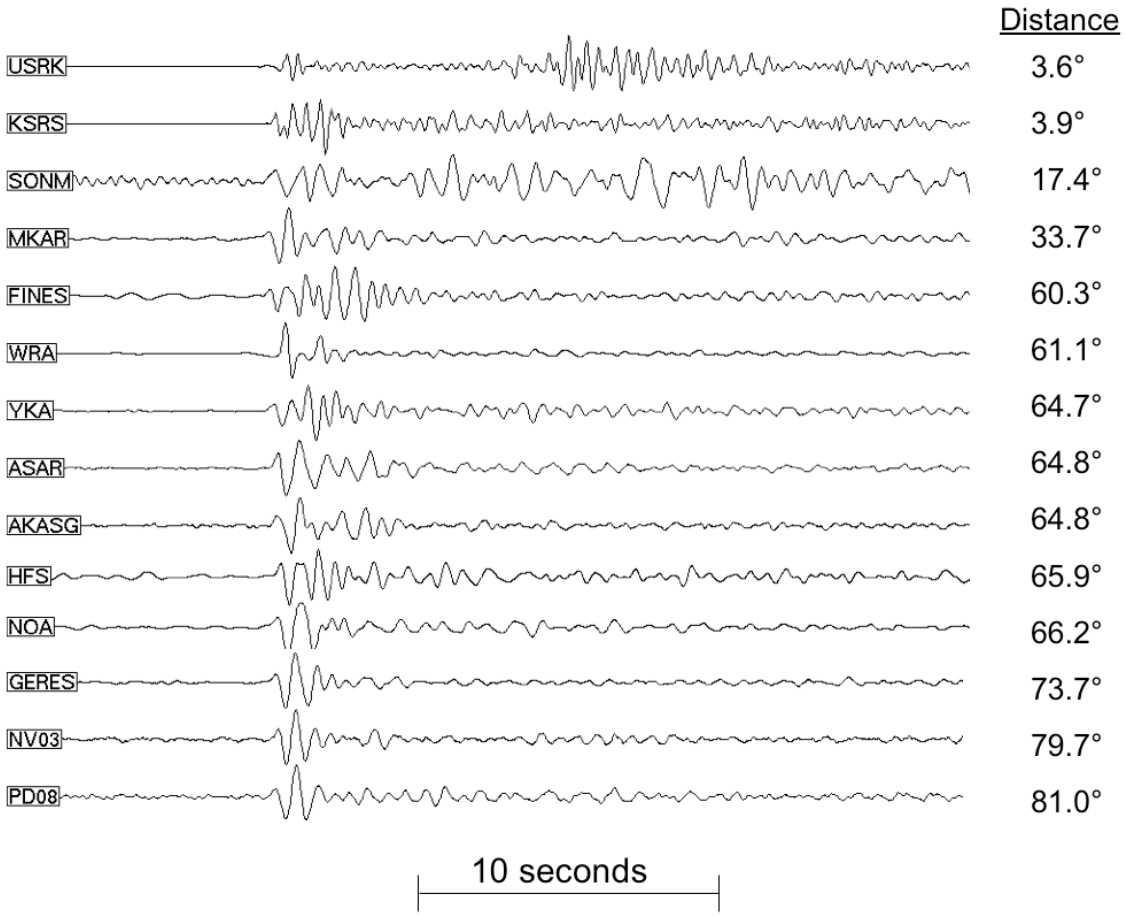

Figure 3. Example of waveform recordings of the May 25, 2009 nuclear test exhibiting good signal-to-noise ratio (SNR) even at remote teleseismic sites.

2 Location

The objective of this part of the study was to obtain a best estimate of the absolute locations and depths of both nuclear tests using seismic location methods. The lack of historical calibration data from the North Korea test site severely limits the accuracy of single event location methods. Even with good regional structure models, biases of several kilometers can be expected.

Our approach was to first determine the relative locations between the events. We used three relative location algorithms which complement each other in terms of the data, earth structure model and objective function (Table 3). These algorithms were somewhat independent and served as consistency checks against one another (Sections 2.1 and 2.2).

In the second stage of our location analysis, we used the relative locations between the events as a constraint to aid in pinpointing the absolute location. We used high-resolution topographic data along with constraints on depth-of-burial and the relative location to derive the most likely absolute locations of the two events (Section 2.3).

Finally we re-applied the relative location algorithms with free-depth constraint to try to quantify the relative depth between the events (Section 2.4).

Table 3. Comparison of Relative Location Algorithms

	Differential Waveform Interfermetry (DWIF)	Joint Hypocenter Determination (JHD)	Double Difference (DD)
Stations	0 - 85 degrees	0 - 85 degrees	< 10 degrees
Phases	Regional, teleseismic P	First arriving P only	First arriving P only
Travel time model	Source slowness model derived from IASPEI91	IASPEI91 travel time tables	Layered 1-D Korean Peninsula model
Measurements	Waveform cross-correlation	Manual waveform alignment	Manual waveform alignment
Objective Function	"Best" stack of the correlation traces after slowness correction	Weighted RMS residual of measured vs. theoretical after removal of static station corrections	Weighted RMS residual of double-difference times
Algorithm	Snieder and Vrijlandt (2005)	Dewey (1972)	Waldhauser and Ellsworth (2000)

2.1 Waveform Correlation-Based Relation Location

The method builds on the basic concept that the relative location of a new event with respect to one or more reference events can be obtained from differential times of common event-station-phase pairs. Waveform cross-correlation is used to measure the differential times. Rather than pick the lag of the maximum of the correlation trace (which is susceptible to errors due to cycle skipping) to obtain a differential time, the Differential Waveform Interferometry (DWIF) method involves time-shifting the correlation traces for a given event location hypothesis using a slowness model of the source region, and stacking the correlation traces. A grid search is performed to determine the event origin time and hypocenter that maximizes the objective function, here defined as the maximum of the stack.

The individual correlation traces are weighted by the statistical significance of the correlation results, hence event-station-phase pairs that do not correlate well are implicitly down-weighted and no a priori rejection of data or outlier rejection is required. The correlation processing is performed using phase-dependent rules (filter band, window-length) allowing the use of all common body-wave phases (regional, primary, secondary). All stations with waveform recordings and a good SNR signals for both events were used in the processing. This included regional (Pn and some Lg) and teleseismic (P) data.

Results of the first phase of the algorithm, namely the waveform cross-correlation processing (using the October 9, 2006 signals as templates) are shown in Figure 4. It plots the individual cross-correlation results aligned with zero relative lag, i.e. it represents the assumption that both events were at the same location. The vertical bars show the peak in the correlation trace for each station-phase, red indicating a high-level of significance of the correlation peak. High significance is defined as being 99% confident that the null hypothesis can be rejected, i.e. that the correlation result could not have been obtained from the correlation of noise with noise. It is clear from the figure that the correlation traces do not align, indicating that the events were not at the same location. In the second phase of the processing, the individual correlation traces were time-shifted using a source slowness model, according to a relative location and origin time hypothesis. The peak of the stack of the correlation traces was used as the objective function. A grid search was performed for all relative locations and origin times to maximize the objective function.

Figure 5 shows a slice through the objective function grid at fixed relative depth = 0. The breadth of the peak is controlled by the frequency content of the waveform data. To assess the uncertainty in the solution we performed a bootstrap experiment. For each case we randomly selected half of the stations and performed the relative location using the same approach as for the full station network. The locations for each of those cases are plotted as small white "+" symbols. The error ellipse plotted in Figure 5 was defined as the ellipse that enclosed 90% of the bootstrap experiment locations. Figure 6 shows waveform cross-correlation traces aligned after being time-shifted based on the relative location result. The RMS residual in the peaks of the correlation traces was reduced from about 0.160 seconds to 0.023 seconds. To gain further confidence in the result, we applied the algorithm to various subsets of the network. At this stage of the processing the location of the October 9, 2006 event held fixed to the best absolute location reported by Bennett et al. (2006). Table 4 summarizes the results for the various station subsets.

Table 4. Locations of the May 25, 2009 event using DWIF algorithm for various subsets of stations, relative to the Bennett et al. (2006) location for the October 9, 2006 event.

Network	Time of 2009/05/25	ΔEast (km)	ΔNorth (km)	Lat	Lon	N-Sta
IMS, IRIS reg + teleseismic	00:54:45.17	-2.3	0.5	41.2955	129.0575	47
IMS, IRIS, NIED, regional and tele.	00:54:45.17	-2.3	0.5	41.2955	129.0575	87
IMS, IRIS first P only	00:54:45.18	-1.8	0.8	41.2982	129.0635	32
IMS, IRIS regional only	00:54:45.17	-2.4	0.5	41.2955	129.0563	16
IMS, IRIS, regional only, using high-frequency filters	00:54:45.18	-2.2	0.4	41.2946	129.0587	16
IMS, IRIS, NIED, regional only	00:54:45.17	-2.3	0.5	41.2955	129.0575	56

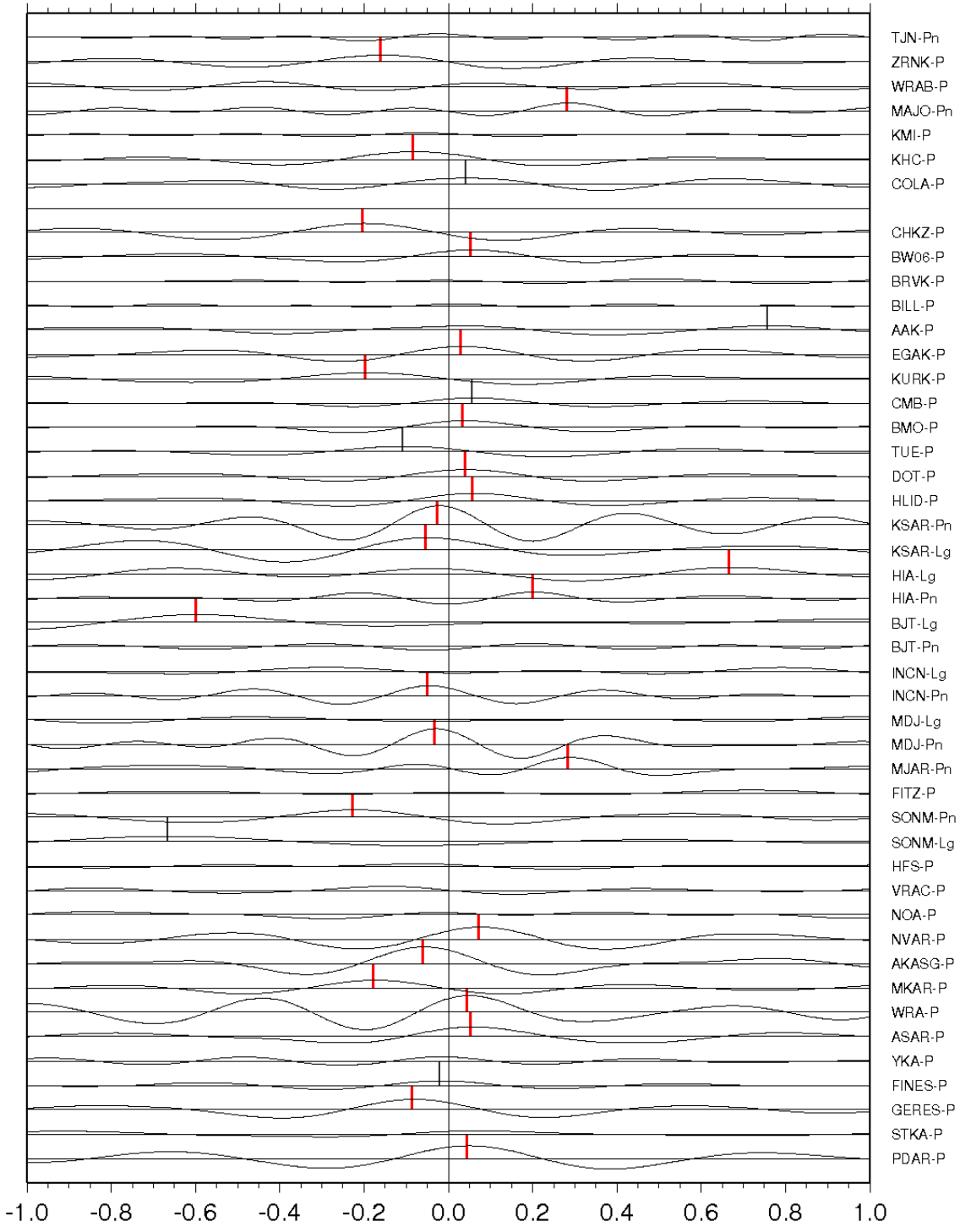

Figure 4. Correlation traces using the October 9, 2006 records as templates. The correlation traces are aligned on zero relative lag, i.e. aligned as though both events occurred at the same location. The correlation traces are scaled by the significance of the peak correlation. The vertical bars mark the time of the peak correlation (red for highly significant results).

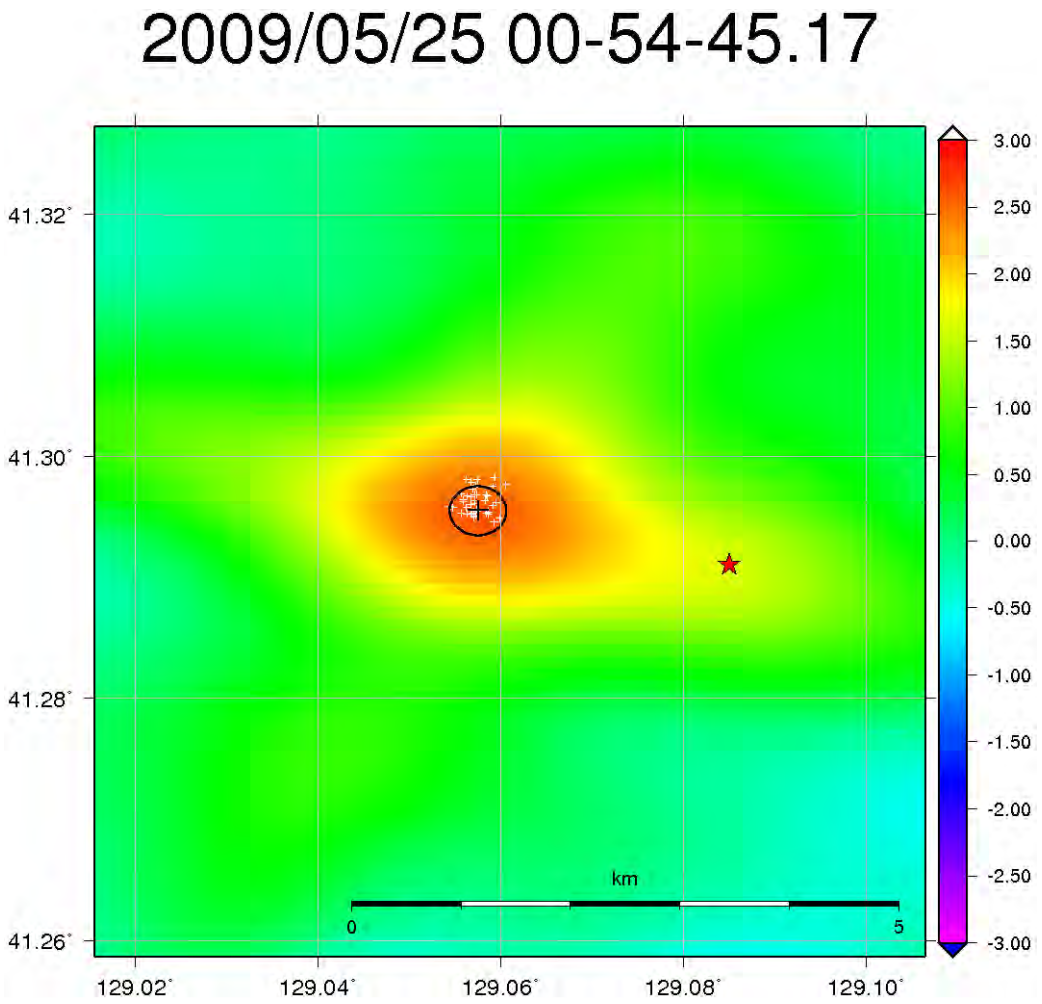

Figure 5. Color-contoured slice through the 3-D objective function grid at constant relative depth (0) at a fixed origin time. The red star marks the location of the October 9, 2006 that was used a fixed reference point in the algorithm. The black "+" marks the best location and the white "+" mark the results of a boot-strap experiment involving subsets of stations to quantify the uncertainty. The black ellipse represents a 90% confidence ellipse based on the bootstrap results.

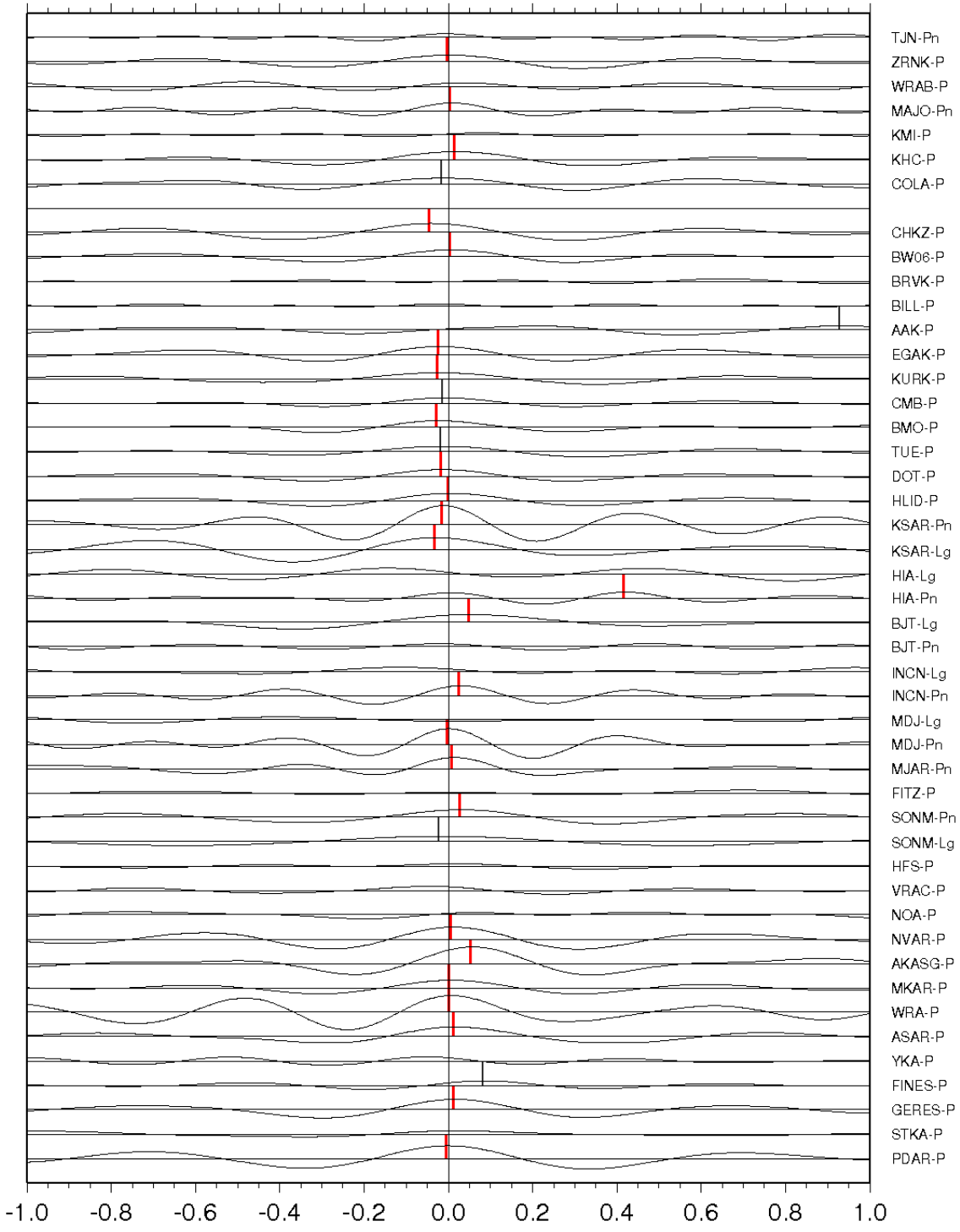

Figure 6. Correlation traces using the October 9, 2006 records as templates. Here the correlation traces are aligned after time-shifting according to the best relative location solution (Figure 5). The highly consistent alignment of the traces for the entire network provides visual confidence to the solution.

2.2 Waveform Alignment and JHD, DD

Waveform Alignment

Relative arrival times for two events recorded with adequate SNR at a given station can often be measured precisely by waveform alignment either manually or with cross correlation (see e.g., Fisk, 2002). We measured such relative arrival times manually for all stations with recordings of both explosions. Data were pre-filtered with a band-pass typically between 1-2 Hz at most stations beyond regional distances to improve SNR. Alignment focused on the initial part of the signals to reduce possible bias due to the 0.4 magnitude difference between the two explosions.

Relative arrival time measurements were made for 56 stations at distances between about 3.5-85 degrees from the North Korean test area. Figure 7 compares aligned signals from the two explosions at four stations. The signals of the 2009 event (in red) appear ever so slightly (20 - 60 ms) delayed relative to those of the 2006 event (in blue) already a couple of cycles after signal onset. This delay effect was observed on waveforms at many stations. This could be an effect of the differences in source spectra between the two explosions; from the larger 2009 event one would expect the lower frequency signal content to be higher than for that of the smaller 2006 event. Cross correlation based on a data-window of several cycles would presumably average the delay and give relative arrival times slightly different from those measured from alignment of the very initial cycle. Figure 8 shows the initial part of the waveform sections in Figure 7. The difference in arrival times for the station-phase pairs (differential times) picked in this manner were very consistent. Figure 9 plots the residual of the differential times with respect to the average differential time. It shows that the picks for the 2009 event for stations in the north-west quadrant are systematically early relative to the 2006 arrivals, indicating that the 2009 test must have been located to the northwest of the 2006 test.

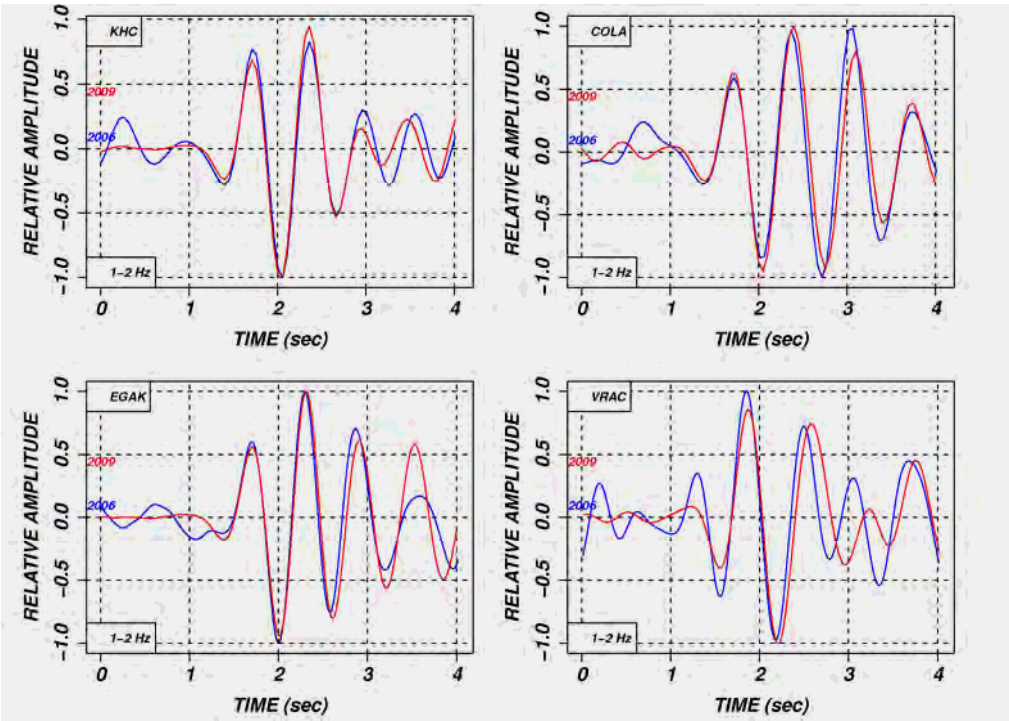

Figure 7. Waveforms for the two explosions at four stations manually aligned.

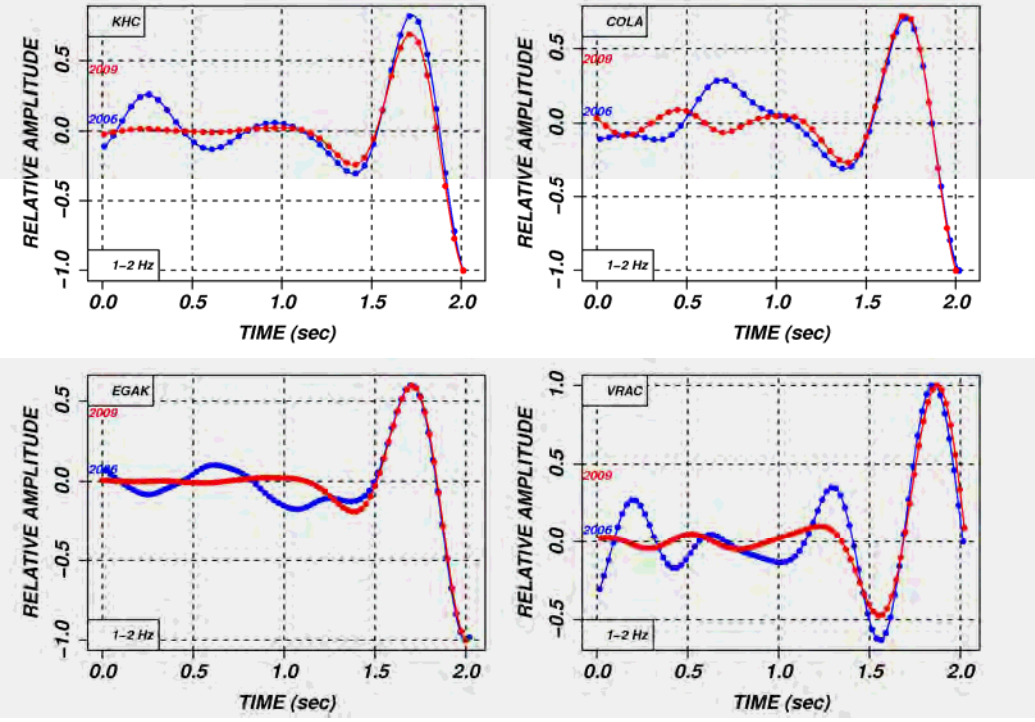

Figure 8. Zoomed in version of Figure 7. Sampled data points are indicated as circular dots.

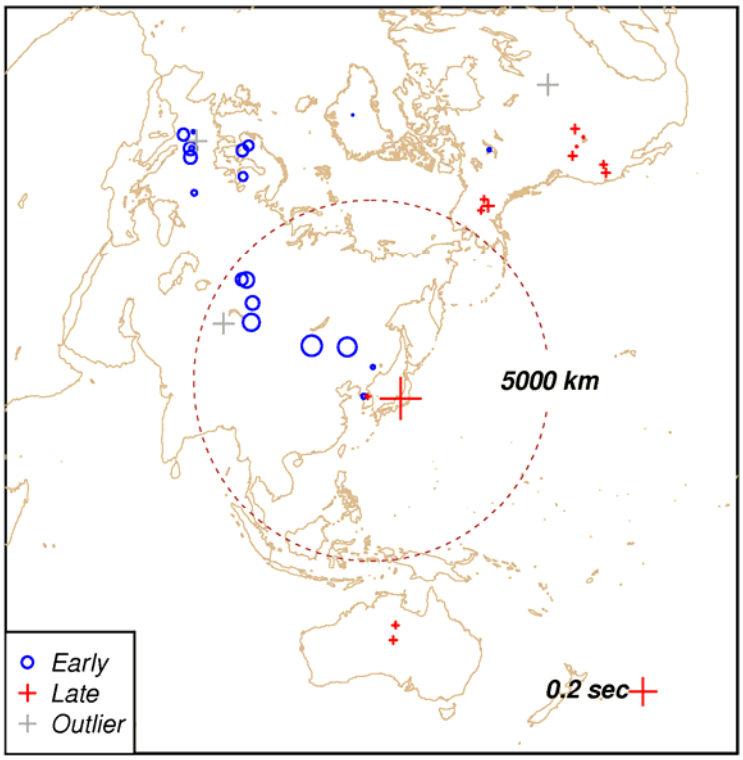

Figure 9. Residuals of the differential times plotted for the IMS and IRIS stations. The early arrivals for the stations to the northwest support the conclusion that the 2009 event occurred to the northwest of the 2006 event.

Joint Hypocenter Determination (JHD)

We calculated relative epicenters of the two explosions using the algorithm (jhd89) developed by Dewey (1972). Apart from epicenters with associated 90% confidence ellipses this algorithm also estimates station corrections and standard deviations of measurement errors of individual phases. Only first arrival P phases were used.

The epicenter of the 2006 explosions was fixed at 41.291 N and 129.085 E and at zero depth (Bennett et al, 2006) throughout the calculations. If this "ground truth" epicenter is mis-located the epicenter of the 2009 explosion will be shifted in a similar way.

Although care was exercised to manually measure relative arrival times, significant errors are sometimes inescapable. Clock errors or other instrumental problems can introduce gross errors in the measured arrival time data. To detect and remove possible gross errors in the data we applied Grubbs' outlier test (Grubbs, 1950). This test, which assumes normality of the underlying distribution, tests the null hypothesis that there are no outliers in the data set. The test was applied iteratively to the arrival time residuals of successive JHD runs. Grubbs' test detects one outlier at a time. Arrivals for the stations with an outlying residual (p-value larger than 0.05) were removed in each iteration before the next JHD run with the arrivals of the remaining stations. This iteration continued until no outlying residuals were detected.

The JHD algorithm with outlier rejection was applied to different combinations of station networks. In addition to stations from the IMS and various IRIS networks, we obtained data from the National Research Institute for Earth Science and Disaster Prevention (NIED) – a network of over 40 stations in Japan (Figure 10), all within regional distance of the North Korean nuclear test site.

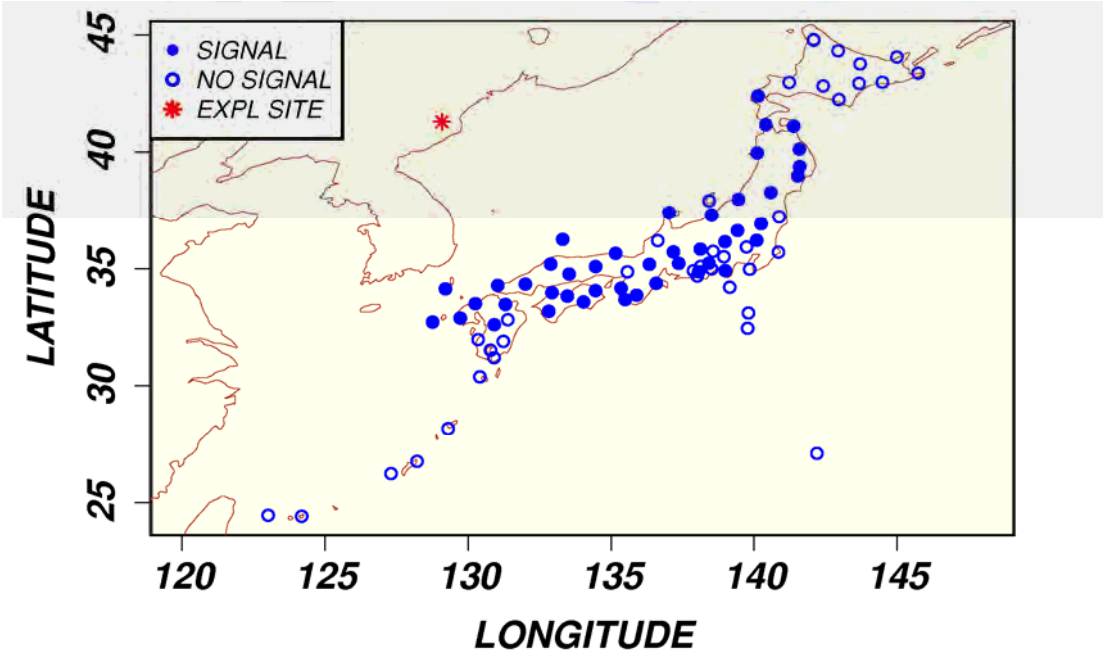

Figure 10. Stations of the NIED network. Stations with good signals for both events are colored with solid blue circles, open circles otherwise.

Table 5 summarizes the results for these JHD runs all employing the IASPEI91 travel time tables. The epicenters of all solutions are, as expected, very close. The solution based on NIED data, i.e., stations only in Japan with azimuths between about 90 and 180 degrees from the explosion sites, is less than 1 km away from the other solutions. The NIED solution has, however, a large uncertainty.

The estimated standard deviations of the measurement errors is about 25 ms and a little higher for the NIED data. The waveforms at most NIED stations, located between 7-10 degrees from the explosions, were usually difficult to correlate due both to high frequency content and complicated propagation paths. The depth was held fixed at zero for both explosions for all cases except for one case using all available data, for which the 2006 depth was fixed at 0.12 km while the 2009 depth was estimated to 0.5 km. The estimated epicenters between the cases of fixed and free depth for the 2009 explosion with all available data are within 0.001 km.

Double Difference (DD) Locations

We apply the double difference method using the hypoDD software (version 1.1) (Waldhauser and Ellsworth, 2000). HypoDD is designed for local data for which a horizontally layered crustal model is specified. For other applications, the DD method has been applied with data out to teleseismic ranges (Waldhauser et al, 2004), but the algorithm is not generally available for this case, which is far more complicated as teleseismic data are more difficult to handle (Waldhauser, personal communication, 2009). Nonetheless we formally applied the hypoDD 1.1 software to data at stations within about 10 degrees. The software package hypoDD 1.1 estimates hypocenters, depth as well as epicenters. Convergence of the calculations were found to be dependent on the depths of the starting solutions, but epicenters of converging solutions generally agreed with JHD solutions. The epicenter of the 2009 explosion for starting depths at zero for both explosions was 41.2983 N 129.0616 E, after the epicenter solutions of the two explosions were shifted so that the epicenter of the 2006 explosion coincided with the "ground truth" used in the JHD calculations. In all 41 stations were used in this solution after applying an outlier cut-off at 1.96 standard deviations (95%).

Table 5. Comparison of the relative location results. The double difference solution (DD) used regional stations including the NIED stations. JHDNIED used the same stations as the DD run, JHDALL used all stations and JHD used regional and teleseismic IMS and IRIS stations.

Auth	Date Time	Latitude	Longitude	Smaj	Smin	Az
fixed	2006/10/09 01:35:29.90	41.291	129.085	0.13	0.12	90
DD	2009/05/25 00:54:44.90	41.2986	129.0616	0.13	0.12	90
JHDNIED	2009/05/25 00:54:45.30	41.2945	129.0687	0.88	0.22	132
JHDALL	2009/05/25 00:54:45.30	41.2983	129.0608	0.16	0.16	1
JHD	2009/05/25 00:54:45.10	41.2968	129.0605	0.25	0.20	62
DWIF	2009/05/25 00:54:45.17	41.2955	129.0575	0.23	0.26	2

2.3 Topographic Analysis

The relative location computations yielded a relative location of the May 25, 2009 event of about 2.5 km to the west-northwest of the October 9, 2006 event. All computations were based on fixing the October 9, 2006 to the location of Bennett et al. (2006) as shown in Figure 11. Any bias in the location of the 2006 event translates into a bias in the 2009 location.

The fixed location reported by Bennett et al. (2006) was estimated as being about 1 km into the mountain from the known tunnel adit in the direction of maximum relief. This placed the 2006 event directly to the north of the adit. This assumed location of the 2006 explosion results in a location for the 2009 on the other side of ridge from the adit (Figure 11). This seems unlikely and suggests that the presumed location of the 2006 may be biased.

We conducted a topographic analysis of the area using ASTER Global Digital Elevation Model. These terrain data are sampled with a posting interval of 30 m, and an accuracy of 7-14 m making them comparable to NIMA DTED level 2. Figure 12 shows the areas that are consistent with the following assumptions:

- Both events were placed in horizontal tunnels from the suspected adit visible in open source satellite image (e.g. Google Earth)
- The 2006 event was placed with 100 – 300 m of overburden. This assumption was based on several observations:
    - An estimated yield of 1.1 kt, which typically requires at least 130 meters for containment[1]
    - Radionuclides were reportedly detected, suggesting possible shallower emplacement
    - Depth of burial of 200 meters based on Pn spectral ratio analysis (Section 3.1)
- The 2009 event was placed with 350 – 750 m of overburden. This assumption was based on:
    - An estimated yield of 4.6 kt, which typically requires at least 220 meters for containment[1]
    - No radionuclide detection, suggests possible deeper containment
    - Depth of burial of 550 meters based on Pn spectral ratio analysis (Section 3.1)

We derived the potential locations of the 2009 event by selecting the areas with sufficient overburden (blue hatched area in Figure 12) that have positions relative to potential possible 2006 event locations (red hatched areas), as constrained by the relative location results. The result is shown in Figure 13, i.e. the blue hatched area is the **only** area that is consistent with all three constraints:

1. The 2006 event was placed with 100 – 300 m of overburden relative to the adit elevation
2. The 2009 event was placed with 350 – 750 m of overburden relative to the adit elevation
3. The 2009 events was about 2.5 km to the west-northwest of the 2006 event

Much of the hatched area in Figure 14 is beyond the ridge line relative to the adit. Figure 14 shows our best estimate of the locations of both events, along with the relief. This result gives a depth of burial of about 180 meters for the 2006 event and 600 meters for the 2009 event.

[1] Scaled depth ~ 130 * (yield in kT)$^{1/3}$

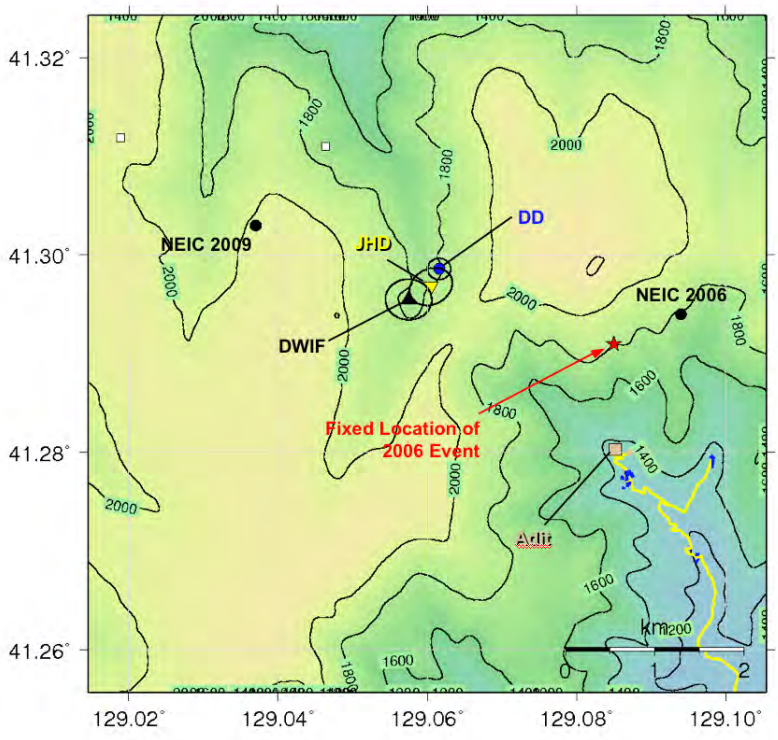

Figure 11. Locations of the May 25, 2009 event assuming a fixed location for the October 9, 2006 event based on Bennett et al. (2006). It places the 2009 event beyond the area of maximum overburden relative to the adit, indicating a probable bias in the fixed location for the 2006 event.

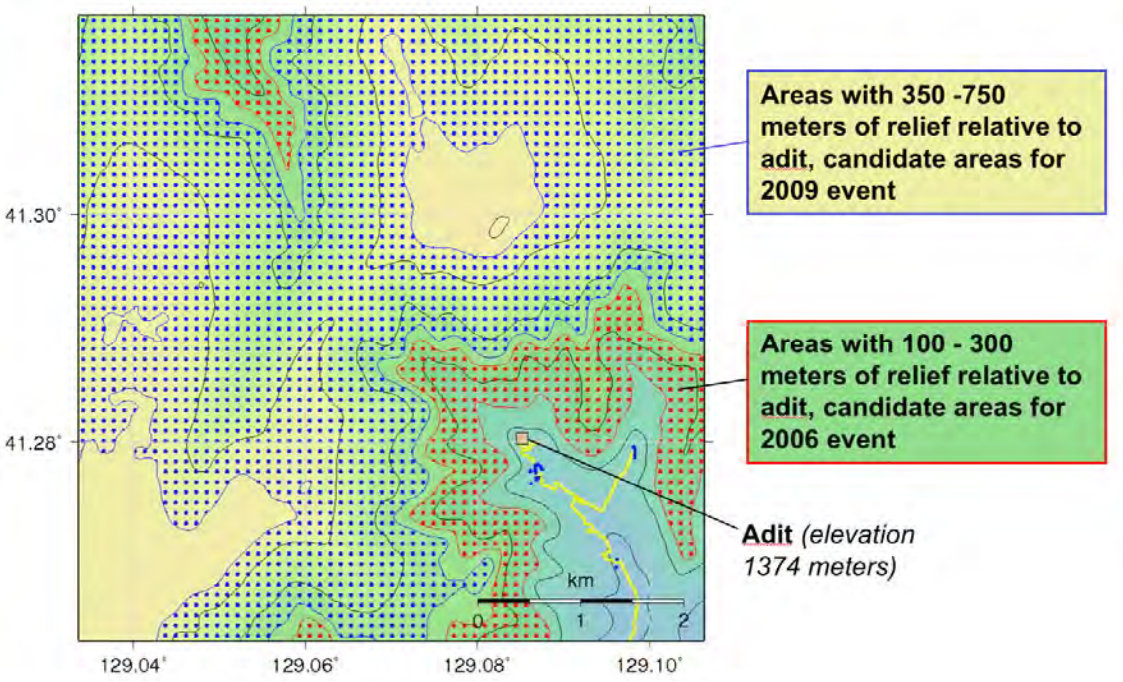

Figure 12. Candidate locations of the 2006 event (red hatched) and 2009 event (blue hatched)

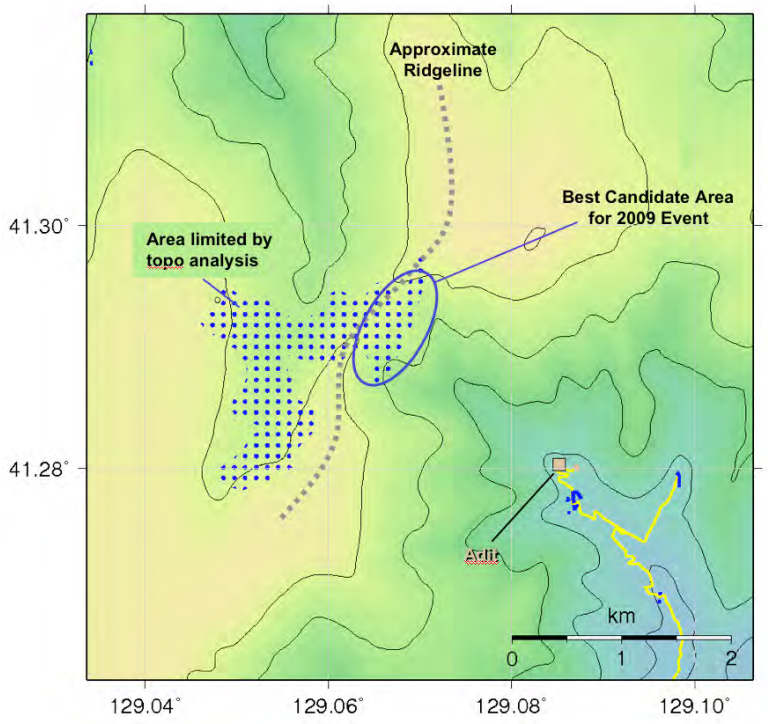

Figure 13. Candidate areas for the 2009 event (blue hatched) constrained by the relief requirements (Figure 12) and constrained by the relative location determined in Sections 2.1 and 2.2.

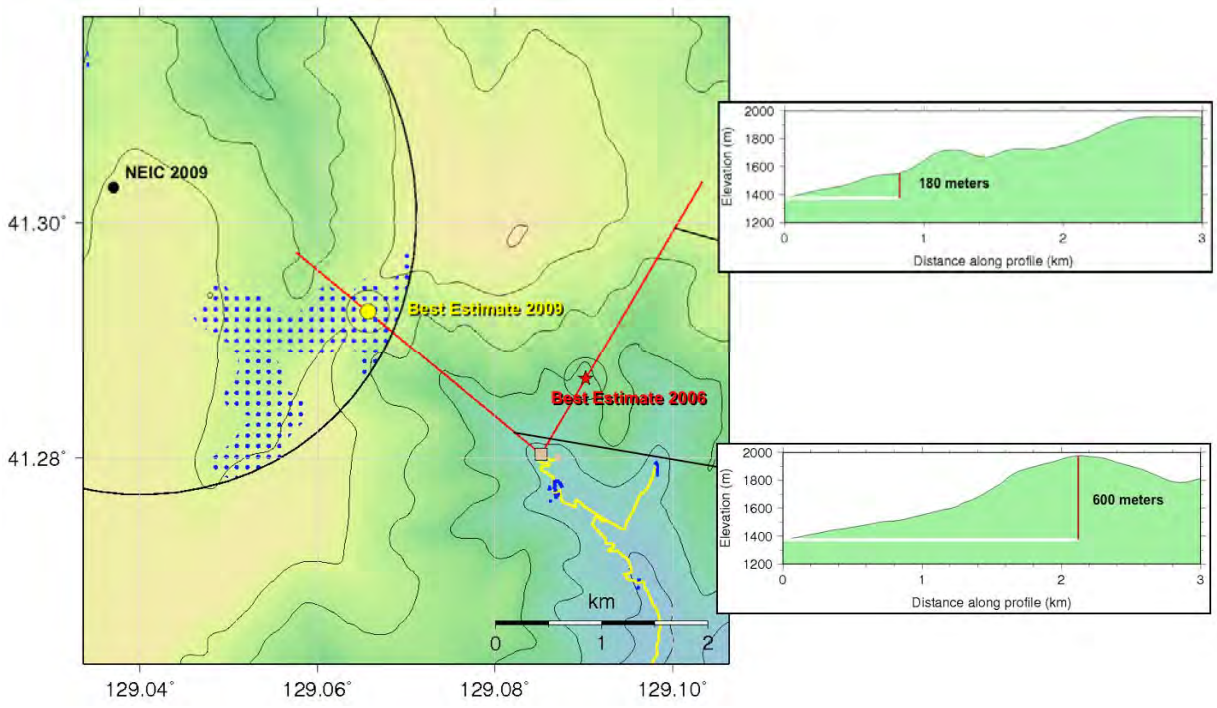

Figure 14. Best estimates for the locations of both nuclear tests resulting from the topographic analysis, assuming that the tunnel for the 2009 event did not go beyond the location of maximum relief.

2.4 Relative Depth

The relative location results presented in Sections 2.1 and 2.2 were performed constraining the relative depth between the two events to 0.0 km. All three methods produced results that reduced the RMS of differential time variations to about 25 milliseconds. The question is whether the remaining scatter in the correlation peaks in Figure 6 on page 9 is due to random timing errors or whether it may still contain information on relative depth.

We applied the same methodology described in Section 2.1 assuming relative depths between -2.0 and +2.0 km in various increments. For each case we searched for "best relative" depth based on both the maximum of the correlation stack and alternately by looking for the minimum of the RMS of the correlation picks (Table 6). The "best" depth estimates range from -0.5 to 0.2 km of the 2009 event relative to the 2006. Given the broad nature of the CC-stack peak and broad trough of the RMS residuals, we conclude that with the current data set this method can provide no more precise depth estimate than that both events occurred within ±500 meters of relative depth.

Table 6. Depth of 2009 event relative to 2006 event using the waveform correlation method for three subsets of stations. The green entries mark the maximum of the correlation stack (same objective function as described in Section 2.1) and the minimum of the RMS of the correlation picks.

Regional Only			P-only		All	
Depth	CC-Stack	RMS	CC-Stack	RMS	CC-Stack	RMS
-2.00	2.5336	0.0682	2.1594	0.0648		
-1.80	2.6820	0.0640				
-1.60	2.8139	0.0603				
-1.50			2.3811	0.0513		
-1.40	2.9077	0.0584				
-1.20	3.0044	0.0493				
-1.00	3.0846	0.0405	2.5260	0.0361		
-0.90	3.1114	0.0432				
-0.80	3.1243	0.0394	2.5585	0.0343		
-0.70	3.1410	0.0356				
-0.60	3.1509	0.0325	2.5827	0.0308		
-0.50	3.1618	0.0351	2.5888	0.0282	1.3127	0.0223
-0.45	3.1642	0.0364				
-0.40	3.1740	0.0313	2.5869	0.0258	1.3155	0.0216
-0.35	3.1714	0.0298				
-0.30	3.1703	0.0285	2.5878	0.0247	1.3167	0.0212
-0.25	3.1711	0.0269				
-0.20	3.1651	0.0258	2.5835	0.0256	1.3163	0.0212
-0.15	3.1661	0.0336				
-0.10	3.1516	0.0326	2.5769	0.0238	1.3169	0.0211
-0.05	3.1569	0.0314				
0.00	3.1427	0.0308	2.5683	0.0230	1.3152	0.0214
0.05	3.1349	0.0304				
0.10	3.1253	0.0298	2.5502	0.0226	1.3162	0.0213
0.15	3.1096	0.0298				
0.20	3.1007	0.0365	2.5368	0.0222	1.3144	0.0215
0.25	3.0836	0.0300				
0.30	3.0720	0.0365	2.5177	0.0247	1.3142	0.0215
0.35	3.0565	0.0320				
0.40	3.0391	0.0319	2.5002	0.0248	1.3097	0.0222
0.45	3.0268	0.0322				
0.50	3.0108	0.0322	2.4750	0.0264	1.3074	0.0234
0.60	2.9709	0.0341	2.4509	0.0267		
0.70	2.9299	0.0360				
0.80	2.8855	0.0386	2.3958	0.0308		
0.90	2.8390	0.0440				
1.00	2.7888	0.0463	2.3390	0.0350		
1.20	2.6950	0.0473				
1.40	2.5899	0.0545				
1.50			2.1791	0.0498		
1.60	2.4731	0.0589				
1.80	2.3712	0.0671				
2.00	2.2646	0.0761	1.9939	0.0629		

3 Yield

3.1 Seismic Yield Estimates Based on Inversion Analysis of the Observed Network – Averaged Teleseismic P Wave Spectrum

The teleseismic P wave data recorded from the May 25, 2009 North Korean nuclear test at stations of the IMS seismic monitoring network have been analyzed using the model-based network-averaged P wave spectral yield estimation procedures summarized by Murphy and Barker (2001). Figure 15 shows a comparison of the observed network – averaged P wave spectrum for the May 25, 2009 explosion with that observed for the previous October 9, 2006 North Korean nuclear test based on data recorded at nine common teleseismic stations. It can be seen that the spectral amplitude levels for the 2009 test are about a factor of four larger, on average, than those observed from the 2006 test over this short-period band extending from 0.5 to 2.5 Hz. The observed network – averaged teleseismic P wave spectrum for the 2009 nuclear test is compared with the corresponding best fitting theoretical predictions obtained using the Mueller/Murphy explosion seismic source model in Figure 16, assuming a source depth of 200m in hardrock and frequency-dependent distance attenuation models appropriate for nuclear tests at the former Soviet Semipalatinsk Test Site (Semi) and the Nevada Test Site (NTS). It can be seen that the yield estimate varies by about a factor of two (2.7 kt versus 5.3 kt) depending on the selected attenuation model and that, in this case, the Semipalatinsk model with an associated yield estimate of 2.7 kt provides a much better overall fit to the observed spectrum over the 0.5 to 2.5 Hz band than does the NTS model. Consequently, the Semipalatinsk attenuation model will be used for all subsequent yield estimation modeling.

The observed network-averaged teleseismic P wave spectrum for the 2009 test is compared with the best fitting predictions for hypothetical Mueller/Murphy sources at depths of 200m and 800m in Figure 17. It can be seen that these two theoretical predictions are essentially identical over the available 0.5 to 2.5 Hz frequency band. That is , the observed teleseismic spectral data do not have the resolving power to distinguish between the alternate hypotheses of a 2.7 kt explosion at a depth of 200m and a 4.8 kt explosion at a depth of 800 m. In fact, these teleseismic data cannot be used to distinguish between theoretical solutions for any depth in the plausible (based on local topographic data and satellite imagery) range extending from 100 to 800m. Consequently, we have estimated the best-fitting theoretical yields at every 100m interval in this range and the results are summarized in Table 7 where it can be seen that they vary from 2.0 kt at 100m depth to 4.8 kt at 800m depth. That is, this range in plausible source depths translates into an uncertainty of about a factor of 2.4 in the associated yield estimate. As is illustrated in Figure 18, this uncertainty range is large relative to any modeling misfit at a fixed depth. Note that in this case, where a fixed depth of 200m is assumed, the predictions corresponding to a range of a factor of 2 in yield completely bound the observed spectral amplitude levels over the 0.5 to 2.5 Hz frequency band, indicating that the modeling uncertainty in yield at a fixed depth is much smaller than a factor of 2. Consequently, in the next section we will attempt to refine the source depth estimate for this explosion and use that depth constraint to obtain a more precise yield estimate.

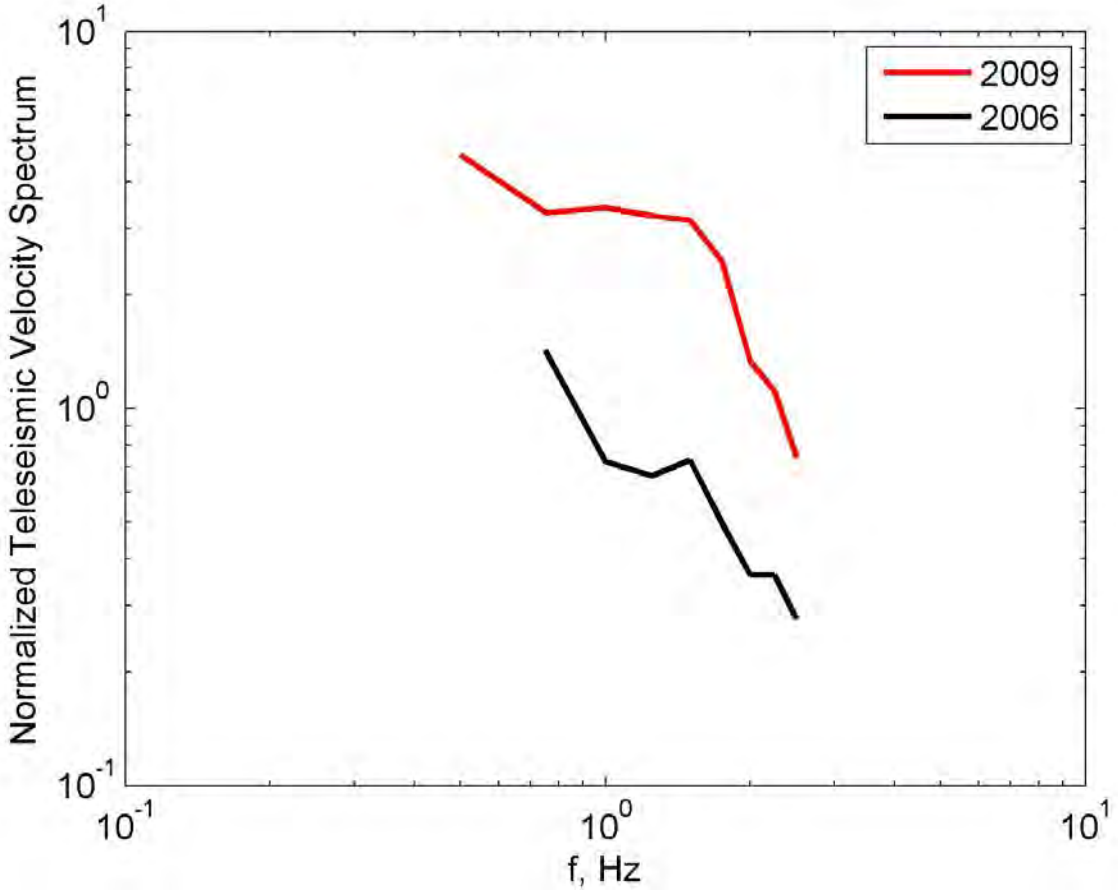

Figure 15. Comparison of the network-averaged, teleseismic P wave spectra determined from data recorded at a common set of stations from the North Korean nuclear tests of May 25, 2009 and October 9, 2006. It can be seen that the spectral amplitude levels for the May 25, 2009 test are about a factor of 4 larger, on average, than those for the October 9, 2006 test over the frequency band extending from 0.5 to 2.5 Hz.

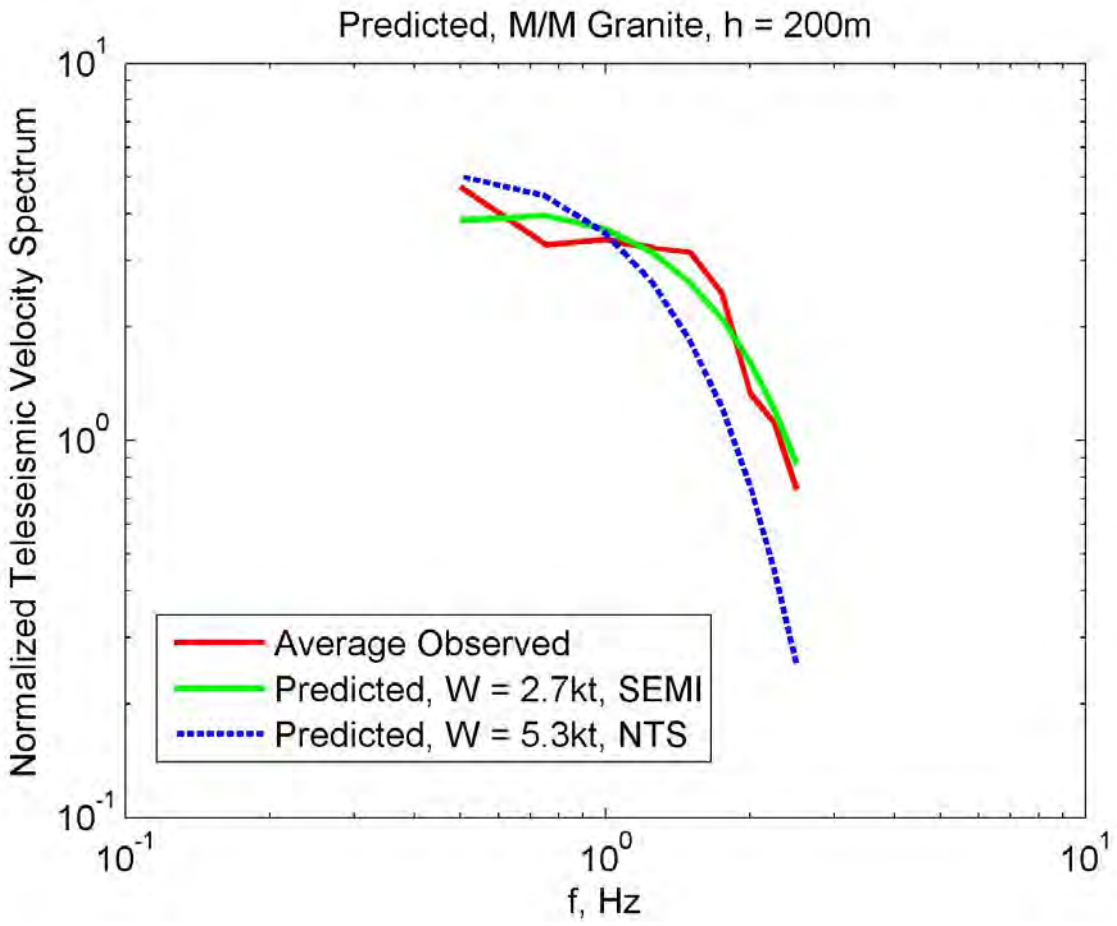

Figure 16. Comparison of the observed network-averaged teleseismic P wave spectrum for the May 25, 2009 North Korean nuclear test with the best-fitting theoretical Mueller/Murphy source models, assuming a source depth of 200m and attenuation models consistent with tests at the Semipalatinsk and NTS test sites. It can be seen that the Semipalatinsk model is much more consistent with the observed spectral data.

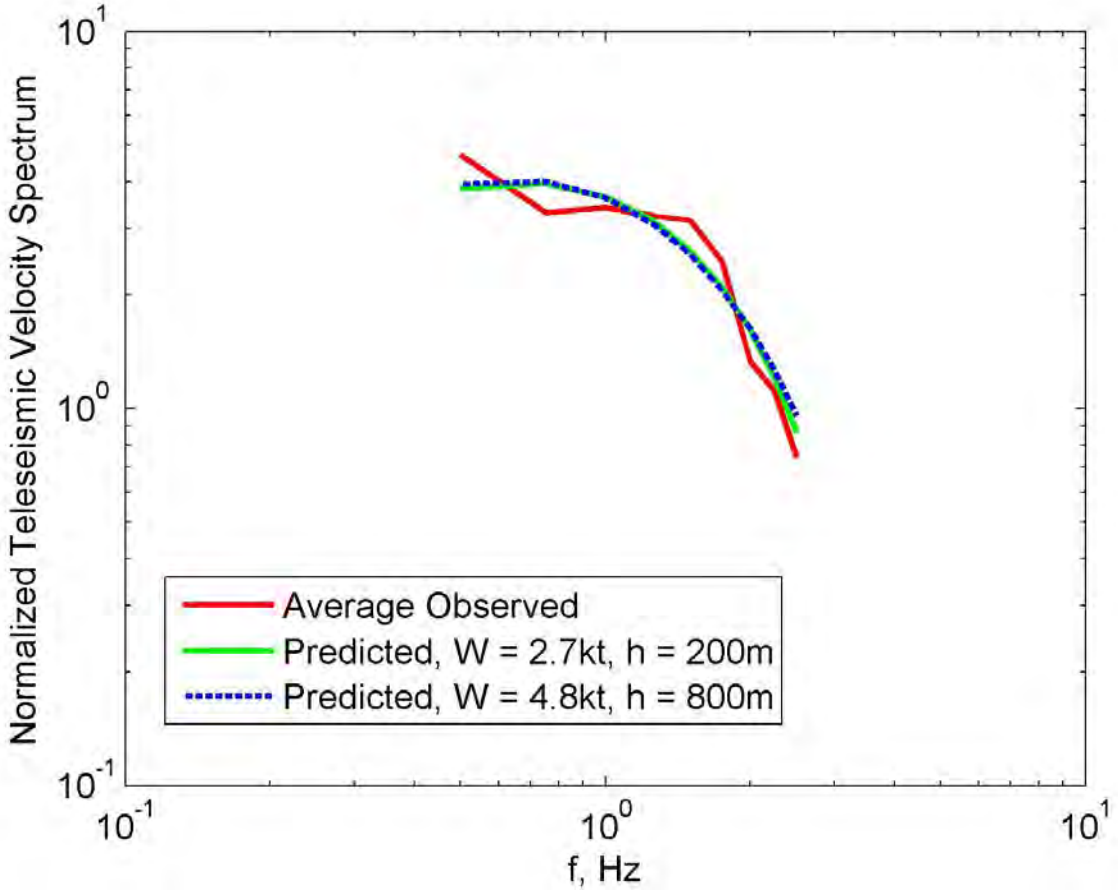

Figure 17. Comparison of the observed network-averaged teleseismic P wave spectrum for the May 25, 2009 North Korean nuclear test with the best-fitting theoretical Mueller/Murphy source models, assuming source depths of 200 and 800m. It can be seen that the observed spectral data do not have the resolving power to distinguish between the alternate hypotheses of a 2.7 kt explosion at a depth of 200m and a 4.8 kt explosion at a depth of 800m.

Table 7. Teleseismic P wave Yield Estimates as a Function of Assumed Source Depth for the May 25, 2009 North Korean Nuclear Test

Source Depth, m	Yield, kt
100	2.0
200	2.7
300	3.2
400	3.6
500	3.9
600	4.2
700	4.5
800	4.8

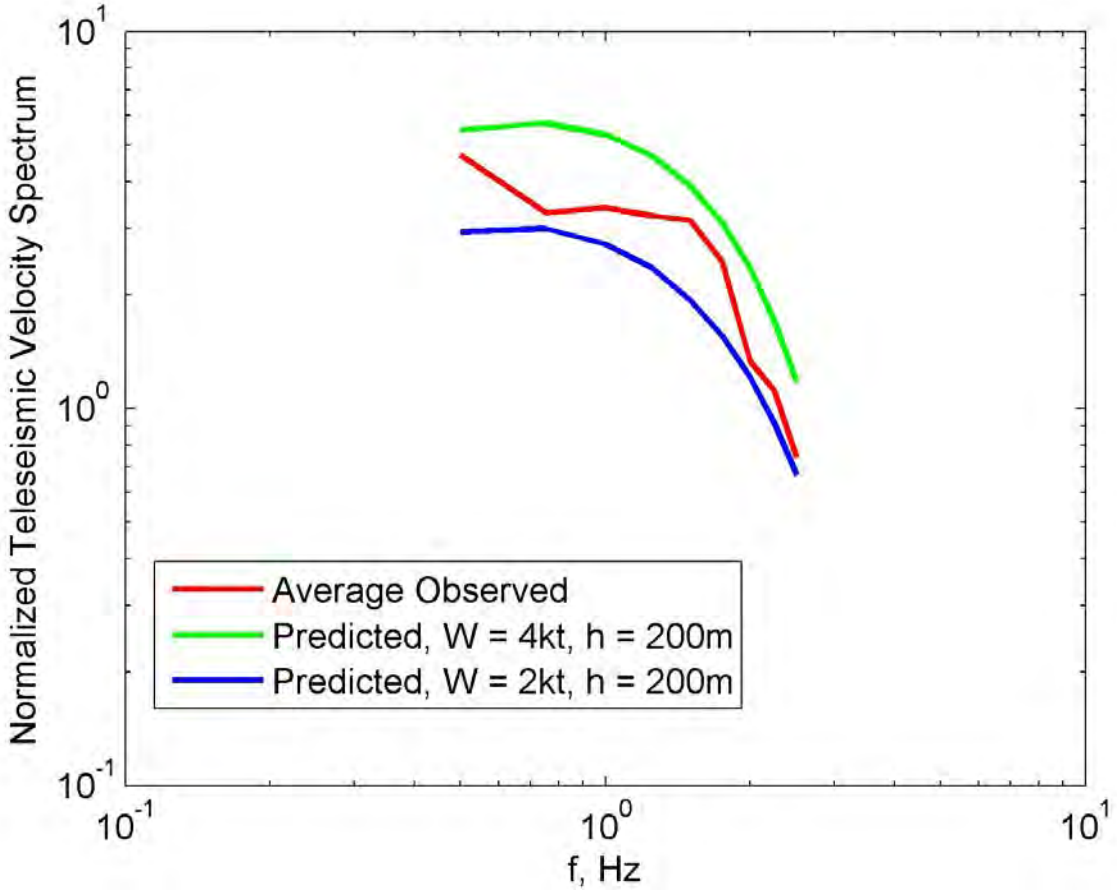

Figure 18. Comparison of the observed network-averaged teleseismic P wave spectrum for the May 25, 2009 North Korean nuclear test with the theoretical Mueller/Murphy source models for 2 kt and 4 kt explosions at a depth of 200m. It can be seen that the predictions for this range of yields at 200m depth completely bound the observed spectral amplitude levels over the 0.5 to 2.5 Hz frequency band.

3.2 Source Depth Estimation for the 2006 and 2009 North Korean Nuclear Tests

As was noted in the previous section, the available teleseismic P wave spectral data over the 0.5 to 2.5 Hz band for the two explosion models do not have the resolving power to distinguish between source depths in the plausible range from 100 to 800m. Similarly, the available seismic phase arrival time data also do not have the resolving power to constrain the source depths in this shallow depth range. This leads to significant uncertainties in the associated seismic yield estimates. Consequently, an investigation was initiated in an attempt to define a robust alternate procedure for constraining the source depths of these two explosions.

In principle, broadband regional P wave data recorded from these explosions can provide the information needed to distinguish between different source depth hypotheses. However, in order to use such data to accurately infer source characteristics, it is necessary to first correct for frequency-dependent propagation path effects, and that cannot currently be done with confidence for the regional distance stations that recorded the two North Korean nuclear tests. One approach to eliminating the uncertainties associated with correcting for frequency-dependent propagation effects is to compute P wave spectral ratios of the two explosions at common regional stations. For these closely-spaced explosions, the propagation path effects are essentially the same, and computing the P wave spectral ratios cancels them out to give estimates of the broadband seismic source spectral ratio between these two explosions. The individual regional station P wave spectral ratios can then be averaged to obtain a robust estimate of the source spectral ratio that can be compared with the theoretical source spectral ratios predicted by the Mueller/Murphy explosion source model corresponding to different source depth hypotheses for the two explosions.

Figure 19. Regional stations used in the Pn spectral ratio analysis.

This analysis procedure has now been applied to the broadband P wave data recorded from the two explosions at regional stations KSRS, MDJ, INCN, TJN and MAJO, whose locations relative to the North Korean test site are shown on a map of the region in Figure 19. The average observed regional P wave source spectral ratio, North Korea (2009)/North Korea (2006) is shown in Figure 20 over the frequency range from 1 to 15 Hz, where it is compared with the theoretical Mueller/Murphy source spectral ratios computed by assuming that both explosions were detonated at the same depth of 200m, or that both explosions were detonated at the same depth of 800m. It can be seen from this comparison that the hypothesis that the two North Korean tests were detonated at the same depth anywhere in the plausible depth range is completely inconsistent with the observed high-frequency spectral ratio data. In fact, it has been found that the observed spectral ratio data are much more consistent with the hypothesis that the 2006 test was conducted at a depth of about 200m, while the 2009 test was conducted at a depth of about 550m. This fact is illustrated in Figure 21 where the average observed spectral ratio is compared with the alternate theoretical Mueller/Murphy source spectral ratio obtained by modeling the 2009 test as a 4.6 kt explosion at a depth of 550m and the 2006 test as a 0.9 kt explosion at a depth of 200m. In these calculations the effects of the surface reflected pP phases were included, with the pP/P amplitude ratios held at 0.3, consistent with previous experience

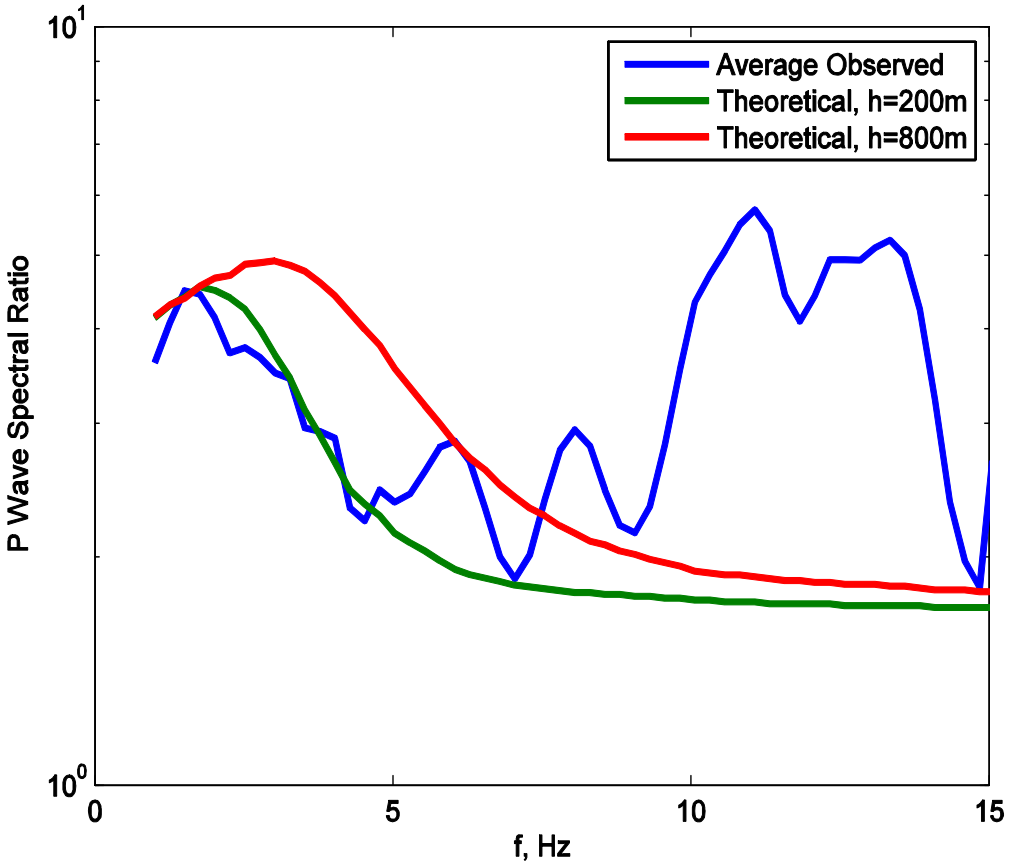

Figure 20. Comparison of the average observed (KSRS, MDJ, INCN, TJN, MAJO) regional P-wave source spectral ratio North Korea(2009)/North Korea(2006) with the theoretical Mueller/Murphy source spectral ratios computed assuming that both explosions were detonated at 200m depth and at 800m depth. It can be seen that the hypothesis that both tests were detonated at the same depth is inconsistent with the observed high frequency spectral ratio data.

with shallow explosions at a variety of other nuclear test sites (Murphy and Barker, 2001). It can be seen from this comparison that these source models predict a source spectral ratio that agrees remarkably well with the average observed spectral ratio over the entire band extending from 1 to 15 Hz. That is, the hypothesis of significantly different source depths for the two North Korean nuclear tests is much more consistent with the observed broadband regional P wave spectral ratio data than is the alternate hypothesis that the tests were conducted at the same depth.

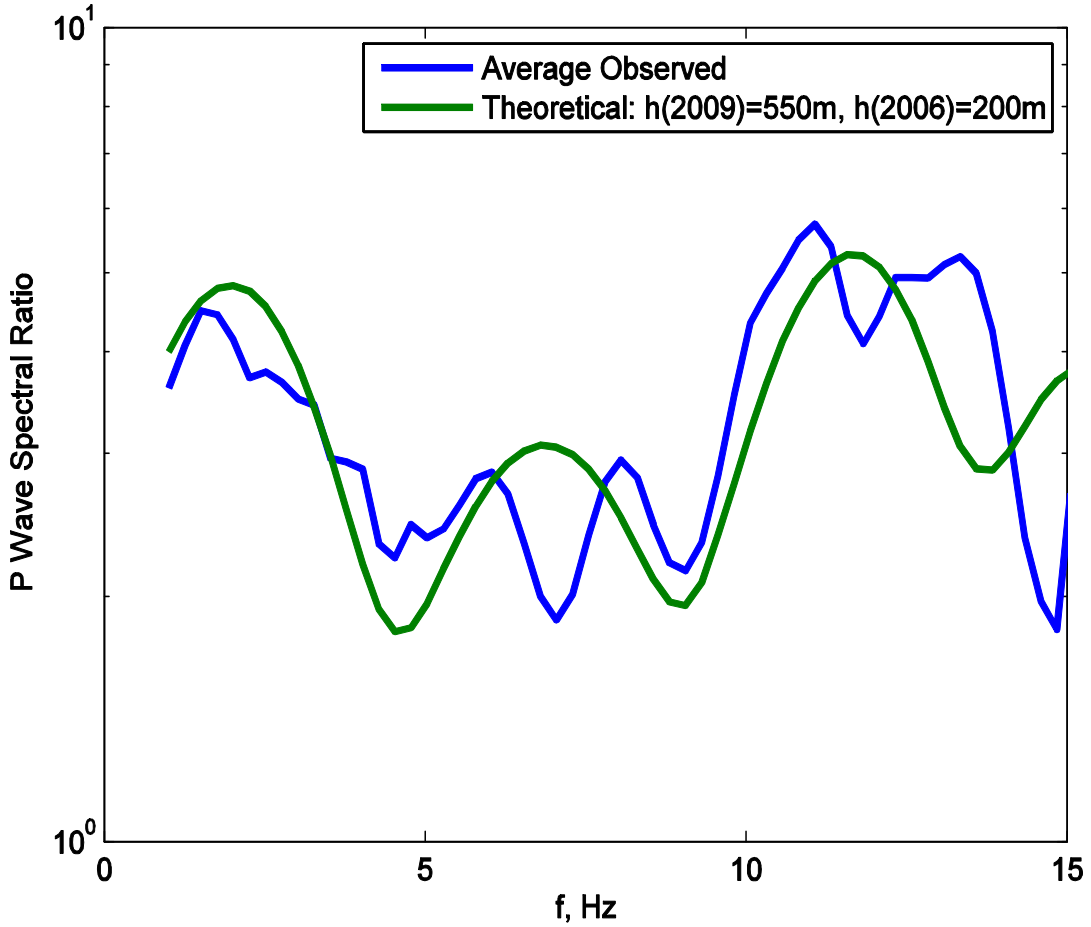

Figure 21. Comparison of the average observed (KSRS, MDJ, INCN, TJN, MAJO) regional P-wave source spectral ratio North Korea(2009)/North Korea(2006) with the theoretical Mueller/Murphy source spectral ratio computed assuming that the 2009 test was conducted at 550m (W=4.6kt), while the 2006 test was conducted at 200m (W=0.9kt), with a pP/P amplitude ratio of 0.3 for both explosions. It can be seen that this hypothesis of significantly different depths for the two explosions is much more consistent with the observed high frequency spectral ratio data.

One remaining source of uncertainty in the above analysis relates to the fact that the observed average spectral ratio at diagnostic frequencies above 10 Hz shown in Figure 20 and Figure 21 above is based on KSRS data alone; and consequently, any undocumented changes in the instrument response at the station between 2006 and 2009 could lead to bias in the estimated high-frequency spectral ratio used to infer the source depths. In order to test for that possibility, we computed 2009/2006 spectral ratios of the pre-signal noise recordings at station KSRS. This spectral ratio is shown in Figure 22, together with a corresponding spectral ratio for station MDJ,

which is the only other of the five regional stations analyzed having a digital sampling rate high enough to support analysis above 10 Hz. Now, while low-frequency noise levels can vary very significantly as a function of time, high-frequency noise levels are generally found to be roughly independent of time, except for occasional isolated narrowband peaks associated with the cultural noise background. Note from the left panel of Figure 22 that the KSRS ratio oscillates around a value of about 1 at high frequencies, consistent with the assumption that the high-frequency instrument response at that station remained constant between 2006 and 2009. On the other hand, the MDJ noise ratio shown in the right panel of Figure 23 indicates a significant decreasing trend with increasing frequency, suggesting some changes in the high-frequency instrument response at that station between 2006 and 2009. Consequently, the average observed P wave spectral ratio above 10 Hz shown in Figure 20 and Figure 21 is based on KSRS data alone. It will be shown in the Appendix that analysis of supplemental near-regional broadband seismic data has confirmed the validity of this KSRS high-frequency source spectral ratio estimate.

Finally, it has been found that the source model for the 2009 test that best explains the observed broadband regional spectral ratio is also consistent with the narrowband teleseismic data. This fact is confirmed in Figure 23 which shows a comparison of the observed network-averaged teleseismic P wave spectrum for the May 25, 2009 North Korean nuclear test with Mueller/Murphy source model predictions for a yield of 4.6 kt at a depth of 550m and a pP/P amplitude ratio of 0.3.

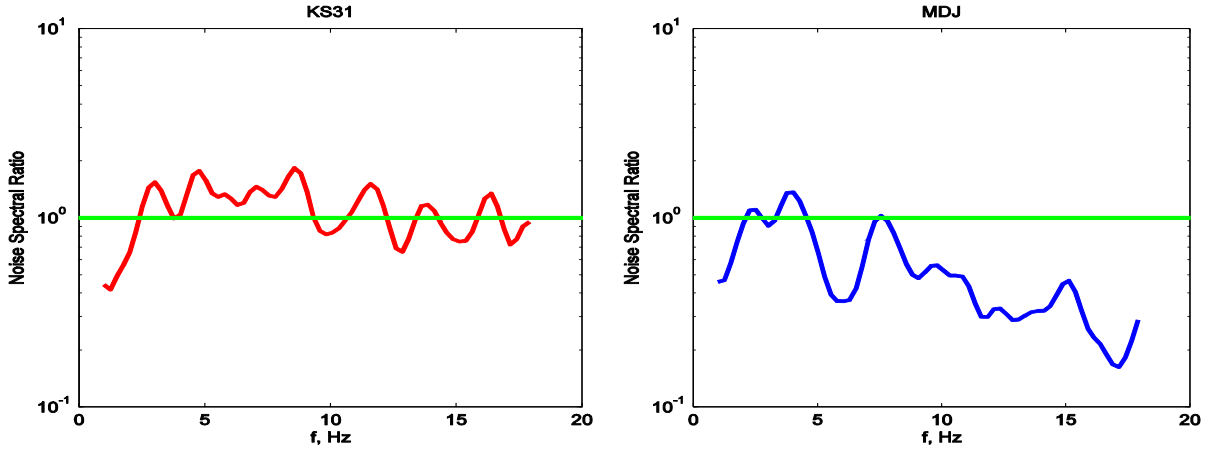

Figure 22. Pre-signal noise spectral ratios, North Korea(2009)/North Korea(2006), for regional stations KSRS (left) and MDJ (right). It can be seen that the KSRS ratio oscillates around a value of 1 at high frequencies, consistent with the assumption that the high frequency instrument response at that station remained constant between 2006 and 2009. However, the MDJ ratio shows a significant decreasing trend with increasing frequency, suggesting some differences in the high frequency instrument response at that station between 2006 and 2009. Consequently, the average observed P-wave source spectral ratio above 10 Hz is based on KSRS data alone.

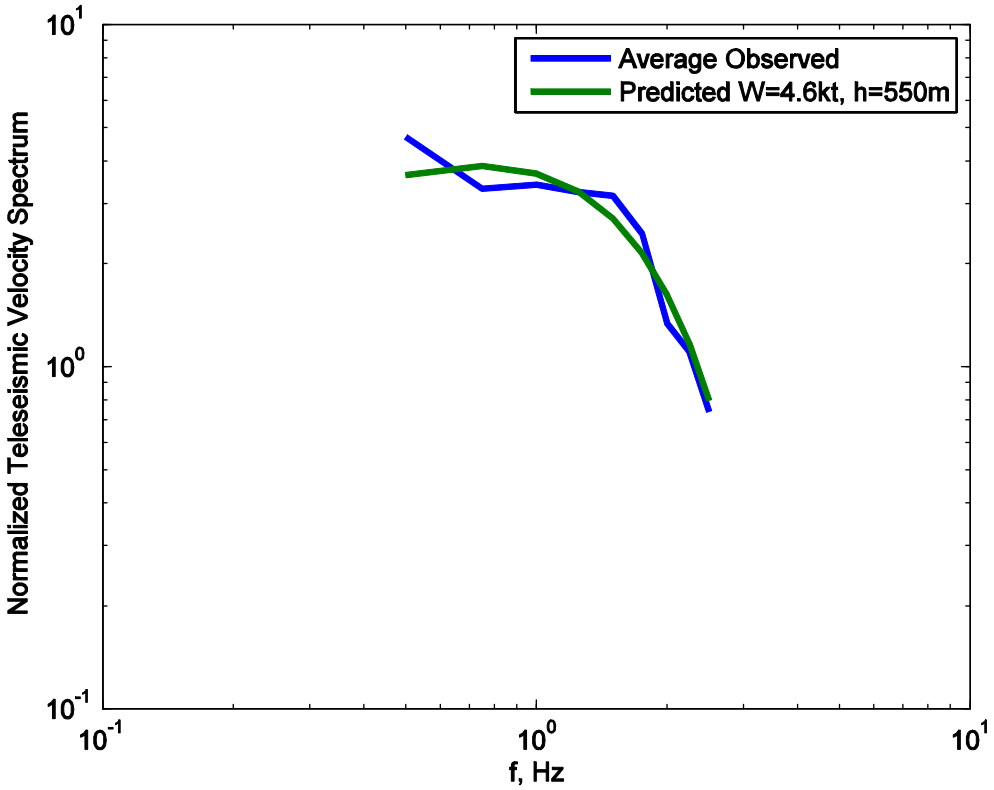

Figure 23. Comparison of the observed network-averaged teleseismic P-wave spectrum for the May 25, 2009 North Korean nuclear test with the Mueller/Murphy source model prediction for W=4.6 kt and h=550m, assuming a pP/P amplitude ratio of 0.3. It can be seen that the source model that provides the best fit to the North Korea(2009)/North Korea(2006) source spectral ratio also provides an excellent fit to the observed network-averaged teleseismic P-wave spectrum for the 2009 explosion.

3.3 Regional mb(Lg) Yield Estimation

Seismic magnitude estimates based on empirical or theoretical explosion scaling relationships are widely used to determine yield. The relationships work best and are believed to produce robust yield estimates for explosions in areas where they have been calibrated to match the results from explosions of known yields. Application or extrapolation of teleseismic magnitude-yield relationships into areas with similar geologic structure where there is no calibration information (e.g. use of Semipalatinsk mb-yield relationship for tests from the Chinese Lop Nor test site) often produces results which look reasonable based on explosion source-scaling models and propagation effects (Murphy, 1996; Stevens and Murphy, 2001). However, for a variety of reasons traditional teleseismic magnitude-yield relationships can sometimes produce divergent yield estimates; and, in the case of the 2009 North Korean nuclear explosion, the traditional relationships provide anomalous results ($W \approx$ 1.2-2.2 kt based on mb = 4.5-4.7 while $W \approx 32$ kt based on Ms = 3.6, assuming yield relationships applicable to platform areas like Semipalatinsk), as discussed elsewhere in this report.

Magnitude measures based on regional Lg and their corresponding relationship to explosion yield (Nuttli, 1986a, b) could potentially provide a useful alternative to estimate explosion size. While Nuttli argued that such magnitudes provided a true estimate of source size, not dependent on local transmission effects (e.g. upper mantle attenuation), and directly relatable to explosion yield, a number of studies since (e.g. Patton, 1988; Priestley and Patton, 1997) have pointed out the need for further calibration of these methods to remove bias effects when extending the magnitude measures and yield relationships into new areas. Extrapolation of mb(Lg)-vs-yield relationships requires careful consideration of how the observed regional phase signals have been biased due to near-source transmission and attenuation differences, which are not accounted for within the magnitude measurement itself.

The USGS/NEIC reported an mb(Lg) magnitude of 3.6 for the 2009 North Korean nuclear explosion based on observations from four stations (INCN, HIA, ULN, ENH). That magnitude corresponds to a very low yield estimate ($W \approx 0.1$ kt), as determined from the Nuttli (1986a, b) mb(Lg)-vs-yield relationships for explosion sources in water-saturated rock. There are a number of reasons to question this result. First, the USGS/NEIC reported the same mb(Lg) magnitude of 3.6 for the 2006 North Korean nuclear explosion; and the earlier test was clearly much smaller. Three stations (MDJ, INCN, MAJO) were used by the USGS/NEIC to determine mb(Lg) for the 2006 event; so, the USGS/NEIC had only one common station between the two events. Furthermore, the USGS/NEIC methodology for determining mb(Lg) utilizes a common attenuation relationship for Lg which is not dependent on the region where the event is located or on the paths specific to the stations where the observations are made (USGS/NEIC, 2010). It seems quite likely that for some of the paths to the stations used by USGS/NEIC to determine mb(Lg) for the North Korean explosions, the effective Lg attenuation could be significantly greater than the one used in the nominal mb(Lg) magnitude formula (e.g. Lg paths to some of the distant regional stations - HIA, ULN, ENH - which recorded the 2009 event or the transoceanic path to MAJO for the 2006 event). In fact, independent studies by Herrmann et al. (1996) and Kohl et al. (2004) both indicate higher attenuation rates for Lg in the Korean peninsula region than the ones used in the USGS/NEIC mb(Lg) magnitude formula, which suggests that the Lg magnitudes reported by USGS/NEIC could be biased low for the North Korean explosions.

To investigate the utility of Lg measurements for use in determining the yield for the 2009 North Korean nuclear explosion, we analyzed observations from six regional stations (Figure 24) at distances 3.3-10.3° which recorded both the 2009 and 2006 explosions. As seen in the map, we did not include regional stations with transoceanic paths (e.g. MAJO in Japan) because of their poor signals, likely associated with Lg blockage.

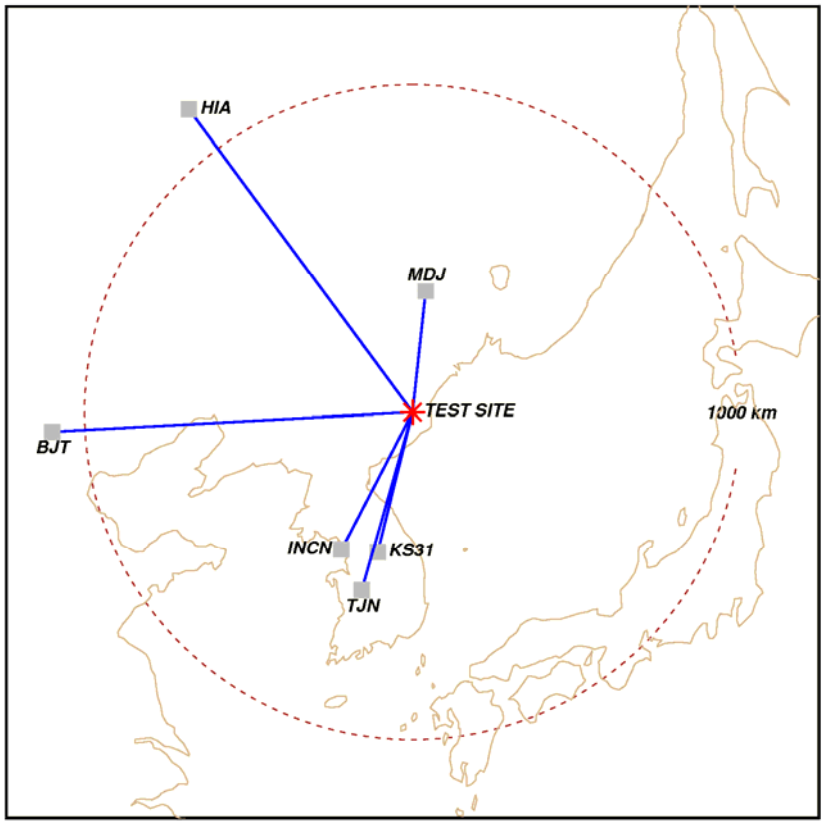

Figure 24. Map showing the locations of six regional stations which recorded Lg signals from both the 2009 and 2006 North Korean nuclear explosions.

At each of the stations we used the broadband (0.8-4.5 Hz) Lg maximum amplitudes measured from the vertical component records in a six-second window starting near the Lg detection time. Because our signal measurements are taken from the broadband records, the associated periods are somewhat shorter (0.3-0.8 seconds) than the nominal 1-second periods normally used for Lg magnitude measurements. To correct for attenuation, we used the relationship developed by Kohl et al. (2004) based on a sample of calibration events from the Korean peninsula recorded at regional stations at distances ~2-20°. The station measurements and their associated magnitudes for both the 2009 and 2006 North Korean nuclear explosions are shown in Table 8. The station mb(Lg) magnitude results in that table show two things: (1) considerable variation in the magnitude measurements between stations with an apparent pattern to the variations, and (2) consistent mb(Lg) magnitude differences between the 2009 and 2006 events at the individual stations.

Table 8. mb(Lg) magnitude measurements from six regional stations which recorded both the 2009 and 2006 North Korean nuclear explosions.

Station	Distance	2006 mb(Lg)	2009 mb(Lg)	Difference
MDJ	3.34	3.49	4.25	0.76
KS31	3.95	3.08	3.66	0.58
INCN	4.25	3.27	3.67	0.40
TJN	5.09	3.29	3.67	0.38
BJT	9.90	3.81	4.24	0.43
HIA	10.33	3.91	4.37	0.47
		3.48	**3.98**	**0.50**

First, with regard to the variation between stations, the mb(Lg) observations from the stations with propagation paths to the south of the North Korean test site (KS31, INCN, TJN) are all biased low relative to the network average, while the observations from stations to the north and northwest (MDJ, HIA, BJT) are all high relative to the average. The most likely cause of this difference is that the Lg signals to the stations in South Korea are subjected to higher attenuation than the Lg signals at stations to the north and northwest. A possible cause of the higher Lg attenuation for the paths to the south is the effect of geologic structure associated with the Imjingang foldbelt (Cho, 2008; Herrmann et al., 2006) which crosses the Korean peninsula (approximately east to west) at about 39°N latitude. The foldbelt represents a major continental collision zone of folding and thrust faulting separating Precambrian massifs with distinct tectonic histories and structure, which would be expected to affect transmission of Lg signals within the crustal waveguide for paths crossing the zone. Since the calibration studies performed by Kohl et al. (2004) involved mainly events and stations with regional propagation not crossing the Imjingang foldbelt zone, they are more likely representative of lower Lg attenuation within a single massif or craton. Although there is need for additional refinement of the details of these propagation effects on Lg magnitude measures for events from the Korean peninsula, it appears that a magnitude bias between 0.3 and 0.8 units would be consistent with the observations at the Southern Korean stations in Table 8.

With regard to the mb(Lg) magnitude differences between the 2009 and 2006 events, the results in the table at all stations show that the 2009 event was larger (by about 0.5 magnitude units on average) than the 2006 event. The differences in station mb(Lg) magnitudes between the 2009 and 2006 explosions range from a low of 0.38 magnitude units at TJN to a high of 0.76 magnitude units at MDJ. If we assume that the slope of the mb(Lg)-versus-yield relationship is 0.76 consistent with the linear fits proposed by Nuttli (1986a, b) and Patton (1988) for water-saturated rock at the explosion source, the average magnitude difference of 0.5 units represents an explosion yield difference of a factor of 4.6 – i.e. the 2009 North Korean test was about 4.6 times greater in yield than the 2006 test. This result is very consistent with the yield estimates for these two explosions determined from the analysis of the regional broadband P wave source spectral ratios presented in Section 3.2 above.

Application of mb(Lg)-versus-yield relationships to determine absolute yields for explosions in the Korean peninsula requires additional work to calibrate the region and to separate transmission effects and Lg attenuation variations. Based on the simple analysis presented above,

it seems likely that removal of the Lg magnitude bias due to station attenuation differences would produce an average network mb(Lg) measure in the range 3.5-3.9 for the 2006 North Korean nuclear explosion and in the range 4.0-4.4 for the 2009 explosion. Estimates corresponding to the standard saturated-rock source relationships would give yields of 0.1-0.2 kt for the 2006 explosion and 0.3-1.0 kt for the 2009 explosion. While these estimates still seem low compared to the more traditional estimates, modest adjustments to account for further effects of near-source Lg transmission could produce somewhat larger yield estimates close to those based on teleseismic P or mb results described elsewhere in this report. Additional work is needed to better calibrate and understand Lg signal transmission, particularly in the near-regional environment specific to the North Korean explosions.

3.4 Surface Wave Detection, Yield Estimation and Discrimination

The two North Korean nuclear tests generated larger than expected surface waves relative to M_s-yield relations derived from historical nuclear explosions. However, the events were somewhat unusual compared to the body of historical explosion surface wave measurements in that they were small and in high velocity hard rock. Most of the historical events are in lower velocity material at NTS, or larger events at both NTS and foreign test sites. A large fraction of the foreign events were at the Soviet Semipalatinsk test site, and many of those events show evidence of compressive tectonic strain release, which has the effect of reducing surface wave amplitudes. So, it is not immediately clear whether the larger surface waves from the North Korean event are highly anomalous, or incorrectly estimated from larger explosions in different media and tectonic settings.

In the following, we examine the Rayleigh and Love waves for these two events, perform a moment tensor inversion to estimate the effect of tectonic release, and compare with predicted results for small explosions in granite.

3.4.1 M_S Measurements

The map locations of the six regional seismic stations (BJT, ENH, HIA, INCN, KS31 and MDJ) that recorded useable long-period data for both North Korean nuclear tests are shown in Figure 25. TLY also recorded the first event. Surface waves were measurable at MAJO, but were strongly affected by the ocean between Korea and Japan, and the data at that station is inconsistent with the other stations in the 10-20 second frequency band. Love Waves were measurable at all six stations for the second event. They were not apparent for the first event, but exist close to the noise level and are visible over limited frequency bands at some stations. In the following analysis we use M_s derived using the Russell (2006) Butterworth filtered surface wave magnitude, which is defined as follows:

$$M_{s(b)} = \log(A_b) + \frac{1}{2}\log(\sin\Delta) + 0.0031\left(\frac{20}{T}\right)^{1.8}\Delta - 0.66\log\left(\frac{20}{T}\right) - \log(f_c) - 0.43 \qquad (1)$$

where A_b is the filtered amplitude, T is the measured period, and f_c is the Butterworth filter width. This equation applies a correction for the frequency dependence of an explosion surface wave source function. The main purpose of $M_{s(b)}$ is to allow surface waves to be measured at regional distances at higher frequencies than traditional 20 second M_s. To the extent that the frequency-dependent source and attenuation functions are correct, equation (1) should be flat with frequency, giving the same M_s value at all frequencies. We applied the same equation to

both Rayleigh and Love waves. Note that for the 2006 test, the Love wave measurements should be regarded as upper bounds as Love waves were close to or below the noise level at all stations. The magnitudes determined for these two events are listed in Table 9.

Table 9. Surface wave magnitudes from North Korean explosions (10-20 second average)

Event	Rayleigh $M_{s(b)}$	Love $M_{s(b)}$
Event 1 – 10/9/2006	2.93 ± 0.20	< 2.58 ± 0.27
Event 2 – 5/25/2009	3.66 ± 0.10	3.07 ± 0.11

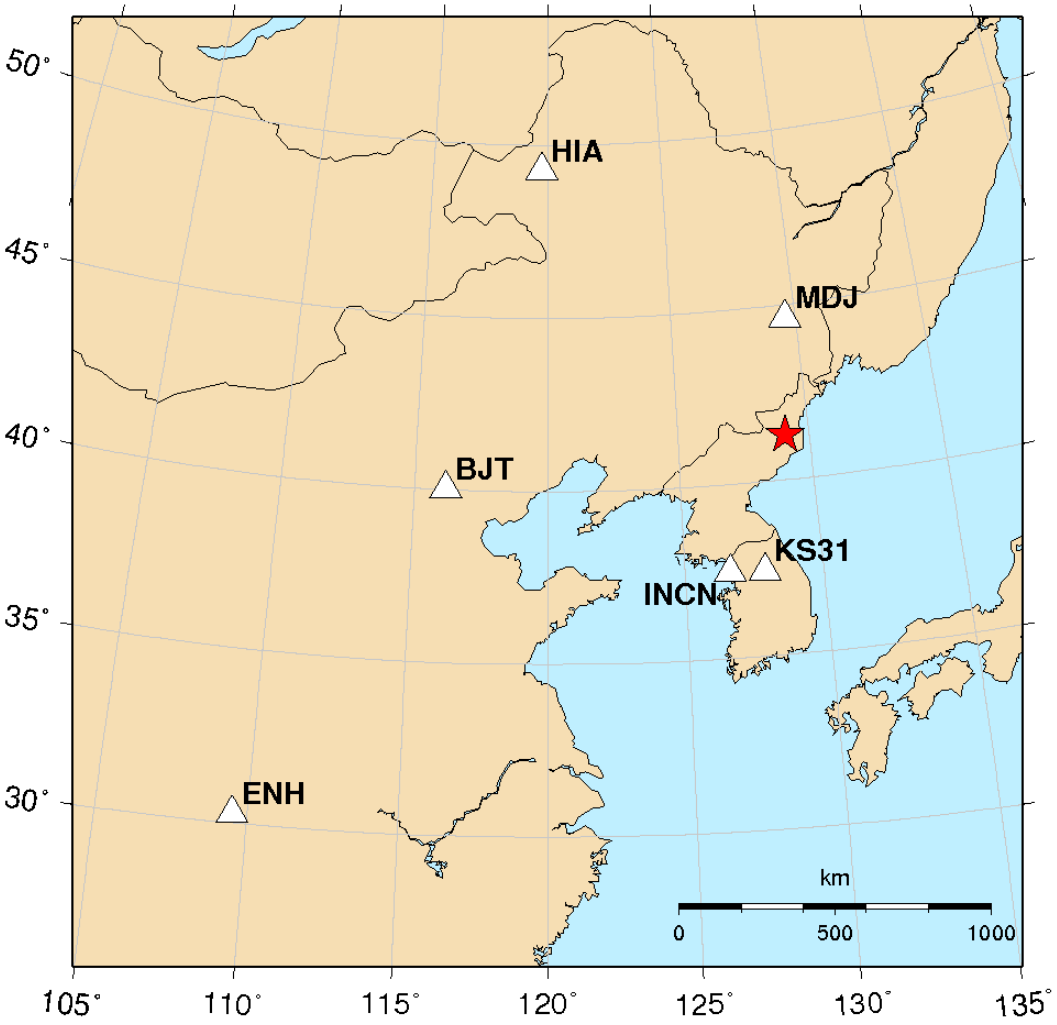

Figure 25. Map locations of the six regional seismic stations that recorded useable long-period data for both North Korean Nuclear tests

3.4.2 Yield Estimation and Discrimination

As was the case for the initial 2006 North Korean nuclear test, the observed M_s value for the 2009 test was found to be anomalously large relative to the corresponding short-period m_b value, providing a seismic yield estimate more than 10 times larger than the short-period yield estimates described in the previous sections of this report. This fact is illustrated in Figure 26 which shows the nominal seismic yield estimates determined from the observed m_b and M_s values. In this

figure the m_b yield estimate (left panel) was obtained using the nominal Semipalatinsk m_b/yield relation, while the M_s yield estimate (right panel) was obtained using the M_s /yield relation

$$Ms = 2.10 + 1.0 \log W \quad (2)$$

derived by Stevens and Murphy (2001) from an analysis of a large, globally distributed sample of M_s /yield observations. The previous observation of a similarly anomalously large M_s value for the initial 2006 North Korean test had led to some speculation that equation (2) might not be appropriate for such small nuclear tests. That is, since equation (2) was derived using data recorded from primarily larger explosions, it was suggested that the M_s /yield slope of 1.0 in (2) might be too large for extrapolating to very small explosions. However, the plausibility of that hypothesis is diminished by the observation that the M_s value for the significantly larger 2009 test is even more anomalously large and much more difficult to reconcile with previous historical observations.

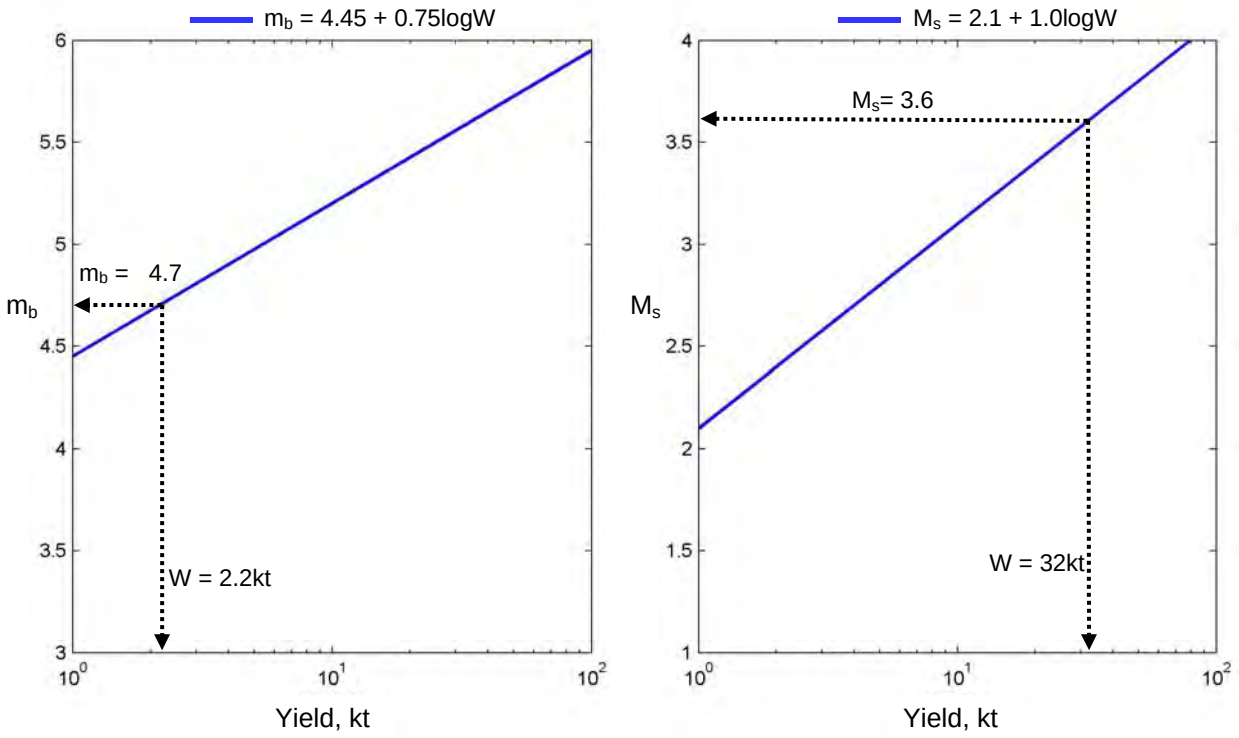

Figure 26. Comparison of nominal seismic yield estimates for the May 25, 2009 North Korean nuclear test based on the observed short-period mb (left) and long-period Ms (right) magnitude measures. It can be seen that the long-period Ms yield estimate is more than 10 times larger than the short-period mb yield estimate.

These apparent M_s anomalies also have implications with regard to the performance of the usually highly reliable M_s/m_b identification criterion, giving indeterminate values for the two North Korean tests that approach previously observed earthquake values. This fact is illustrated in Figure 27 which shows comparisons of the M_s/mb values for the two North Korean nuclear tests with both the nominal event screening line used at the International Data Centre (IDC) for separating earthquake and explosion populations, as well as M_s/m_b values observed from some

recent earthquakes and underground nuclear explosions (left panel). The right panel of this figure shows the observed M_s/m_b values for just the two North Korean tests with respect to the IDC event screening line, where it can be seen that the mean M_s/m_b value for the 2009 test falls on the earthquake-like side of the decision line, while the corresponding value for the 2006 test falls just below the decision line. In both cases, the uncertainties in the M_s/mb value encompass the decision line, so that both are indeterminate; and it is not possible to confidently identify either of these nuclear tests based on the M_s/m_b criterion. Fortunately, as will be shown in the following section, the short-period regional discriminants are effective in this case and they unambiguously identify these two seismic events as nuclear explosions. However, the failure of the normally highly reliable M_s/m_b identification criterion on these two North Korean nuclear tests remains as a troubling unexplained anomaly.

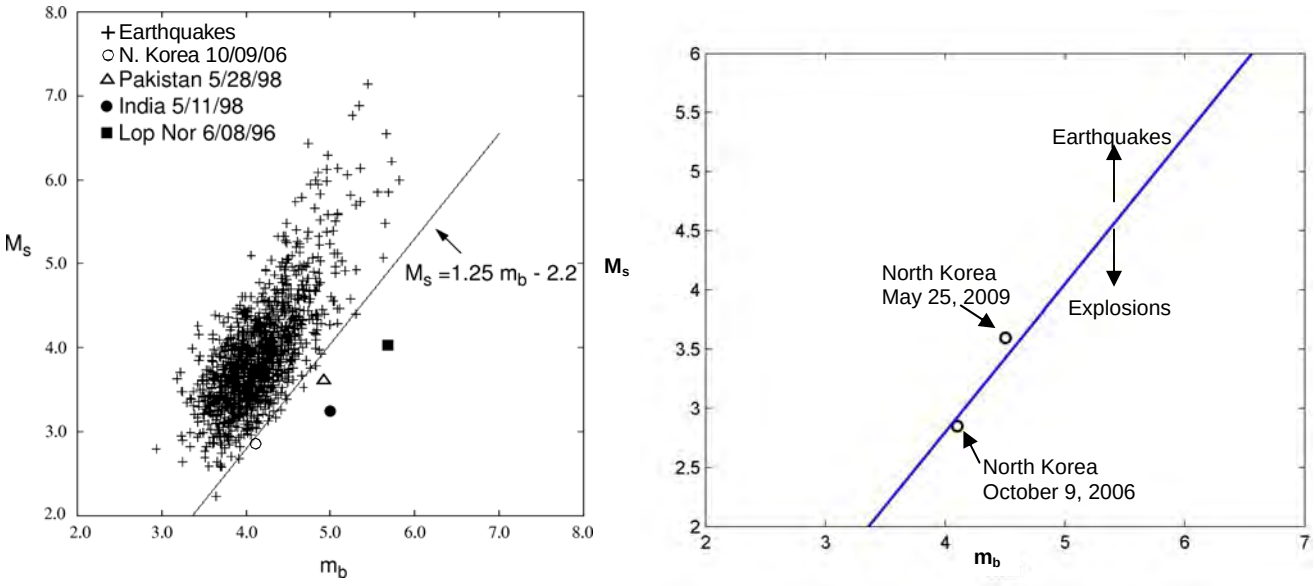

Figure 27. Comparison of the Ms/mb Observations for the North Korean nuclear tests with corresponding Ms/mb Observations from other recent nuclear tests and earthquakes (left). The right panel shows the Ms/mb values for the two North Korean tests with respect to the event screening line used at the IDC,

3.4.3 Analysis of the M_s Anomaly

It was noted above that the observed M_s values for both the 2006 and 2009 North Korean tests were anomalously large and there is evidence to support the hypothesis that the source of these anomalies must be common to both explosions. For example, Figure 28 shows a comparison of the vertical component surface waves recorded at regional station MDJ in China from the two explosions that indicates that the maximum Rayleigh wave amplitudes observed from the 2009 test are about 5 times larger than those observed from the 2006 test, a ratio value that is quite consistent with the observed ratios of the corresponding short-period amplitude data. That is, the differences in the relative long-period Rayleigh wave amplitudes are consistent with the differences in yield inferred from the short-period body wave data, but the absolute M_s values for both tests appear to be biased high. One effect that has been shown to bias M_s values observed from explosions at other test sites is the triggering of the release of pre-existing tectonic strain

energy by the explosion. That is, tectonic strain energy stored in the medium prior to the explosion can be released by the effects of the explosion shock waves, producing a secondary source of long-period surface waves that can either add to or subtract from the direct explosion induced surface waves, leading to anomalous M_s values. Since such secondary tectonic sources are expected to produce long-period transverse Love waves, while pure explosions are not, observations of significant transverse component Love waves on recordings from explosions provides strong evidence for explosion-induced "tectonic release." Thus, it was initially puzzling that the 2006 North Korean nuclear test produced no observable Love waves, despite the fact that the observed M_s value appeared to be quite anomalous. However, clear Love waves were observed from the larger 2009 test; and, if Love waves had been produced by the 2006 test in the same proportion to the observed 2009 Love waves as the corresponding Rayleigh waves, their amplitude levels would have just been below the noise threshold at the observing stations. This fact is illustrated in Figure 29 which shows the transverse recordings at station MDJ for both tests. It can be seen from this figure that the background noise level at this station during the 2006 test was about a factor of 5 below the observed Love wave signal level from the 2009 test. That is, comparable Love waves may have been generated by the 2006 test, but not at detectable levels.

Secondary tectonic release sources are expected to generate Rayleigh waves that show an amplitude variation with azimuth (i.e. a radiation pattern) as well as transverse Love waves. As noted above, these secondary Rayleigh waves can either add to or subtract from the explosion-generated Rayleigh waves depending on the orientation of the tectonic stress field. This fact is illustrated in Figure 30 which shows comparisons of the azimuthal distributions of Rayleigh wave amplitude for explosion plus tectonic release sources versus explosion sources alone for the strike-slip, thrust and normal faulting modes of tectonic release. It can be seen from this figure that the strike-slip mode of tectonic release will generally average out to have a negligible effect on the network averaged M_s value, while the thrust mode of tectonic release will decrease M_s. Thus, for example, detailed investigations of the seismic characteristics of Soviet underground nuclear tests at the Semipalatinsk test site revealed very strong thrust-type tectonic release on some tests that caused the M_s values to be significantly decreased and, consequently, the explosions discriminated very well on the M_s/m_b criterion. However it was noted at the time of the Semipalatinsk analyses that if the sense of the tectonic release was reversed to normal faulting, then the effect would be reversed to increase M_s and make M_s/m_b discrimination more problematic. Thus, accurate characterization of any secondary sources of surface waves is important in seismic monitoring, and moment tensor inversion analysis provides the formalism needed to characterize such secondary sources.

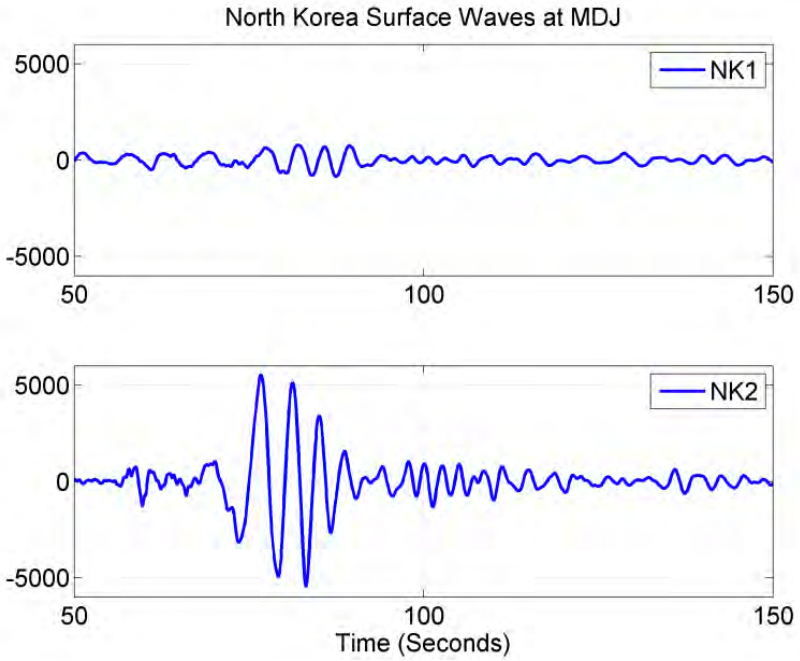

Figure 28. Comparison of long-period vertical component Rayleigh waves recorded at station MDJ from the 2006 (top) and 2009 (bottom) North Korean nuclear tests. The observed amplitude level for the 2009 test is about 5 times larger than that for the 2006 test, consistent with the relative amplitudes of the corresponding short-period P waves.

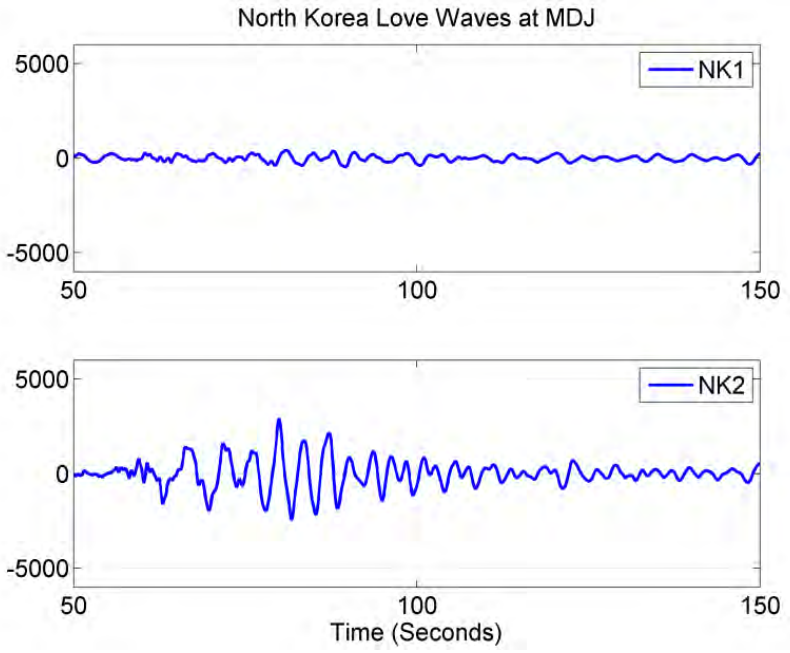

Figure 29. Comparison of long-period transverse component Love waves recorded at station MDJ from the 2006 (top) and 2009 (bottom) North Korean nuclear tests. It can be seen that the noise level at this station at the time of the 2006 test was about 5 times smaller than the signal level for the 2009 test, suggesting that the 2006 Love waves may have been just below the detection threshold.

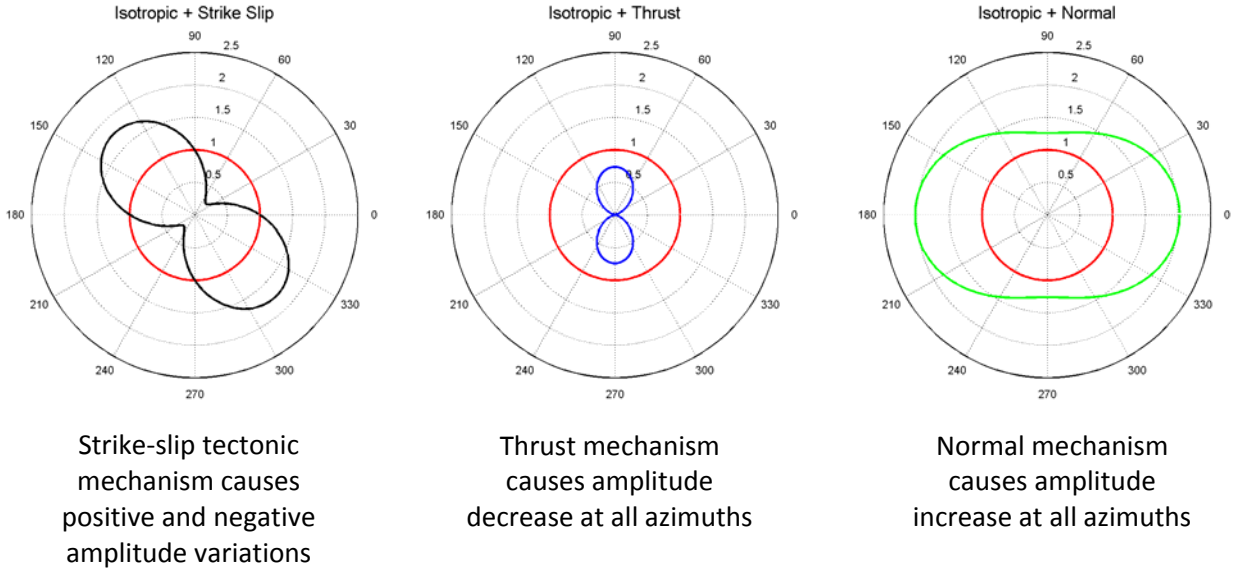

Figure 30. Comparisons of azimuthal distributions of Rayleigh wave amplitudes for explosion plus tectonic release sources versus explosion sources alone (red) for the strike-slip (left) thrust (center) and normal faulting (right) modes of tectonic release.

3.4.4 Moment Tensor Inversion Analysis

The seismic moment tensor is a measure of the near-source displacement field that generates seismic waves. Six independent components of the moment tensor generate different types of motion, all of which add linearly. An isotropic explosion source has identical diagonal moment tensor components and no off-diagonal components.

An explosion is characterized by the isotropic source plus contaminating secondary components which are caused by tectonic strain release or any other near-source factors that cause the source to vary from isotropic. The secondary components may generate Love waves and azimuthal Rayleigh wave amplitude variations. Most analyses of tectonic release from explosions assume that the secondary source can be modeled with a single fault mechanism added to the isotropic source. However, the secondary source is not restricted to a single fault mechanism. Rayleigh waves are generated primarily by the horizontal displacement at the source. A Compensated Linear Vector Dipole (CLVD) source with components Mxx and Myy equal causes the Rayleigh waves to increase or decrease in amplitude uniformly with no Love waves generated. The CLVD source is axisymmetric and is equivalent to two thrust (or normal) faults rotated 90 degrees from each other. As is illustrated in Figure 31, a CLVD compressive in the horizontal directions reduces this displacement at the source and reduces the Rayleigh wave amplitudes. Conversely, a CLVD tensile in the horizontal directions increases the horizontal displacement and increases Rayleigh wave amplitudes.

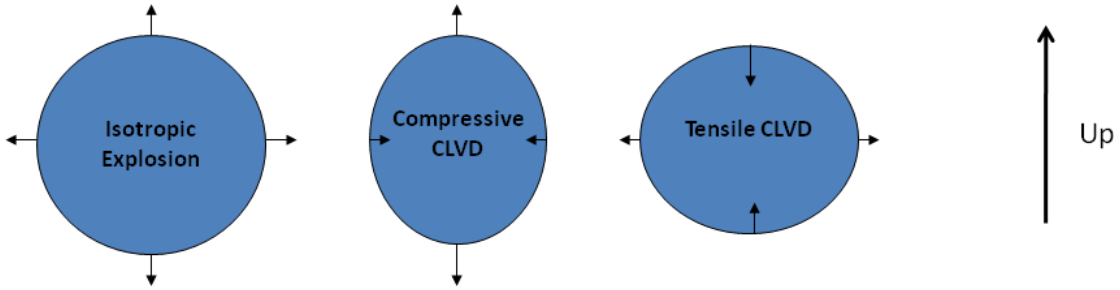

Figure 31. Illustration of the near-source displacements from an isotropic explosion (left), compressive CLVD (center) and tensile CLVD (right). The compressive CLVD reduces Rayleigh wave amplitudes while the tensile CLVD increases them.

To examine the possible effect of tectonic release on surface wave amplitudes observed from the two North Korean tests, we performed moment tensor inversions for the two events. To do this, we performed a search for best fit to all the data in the 10-20 second period band while varying the isotropic moment, CLVD moment and shear moment tensor components, excluding the vertical dip slip moment tensor components which vanish at the free surface. We find the following:

Table 10. Moment tensor inversion results for North Korean explosions (x10^{14} N-m)

Event	Mxx	Myy	Mzz	Mxy
Event 1 – 10/9/2006	4.30	5.56	3.68	-0.50
Event 2 – 5/25/2009	25.12	27.63	18.84	-4.27

Table 11 lists the moment tensor in terms of the isotropic moment $M_I = \left(M_{xx} + M_{yy} + M_{zz}\right)/3$, CLVD defined by $M_{CLVD} = (M_{xx} + M_{yy} - 2M_{zz})/2$, and the shear components. The CLVD as defined here will generate larger surface waves if it is positive, since at shallow depths the horizontal strain is the principal generator of surface waves. The CLVD component is small, but is positive and therefore enhances surface waves.

Table 11. Moment tensor inversion results for North Korean explosions (x10^{14} N-m)

Event	M_I	M_{CLVD}	Mxx-Myy	Mxy
Event 1 – 10/9/2006	4.51	1.25	-1.26	-0.50
Event 2 – 5/25/2009	23.86	7.54	-2.51	-4.27

The Rayleigh and Love wave amplitude spectra over the period band 8 – 25 seconds predicted by these moment tensor solutions for the two North Korean tests are compared with the corresponding observed spectral amplitude data in Figure 32 – Figure 35 where it can be seen that the inversion results provide a reasonable match to the observed data. While details of the spectra differ, the data and calculations have approximately the same average value and spread, and similar relative amplitudes between stations. A notable exception is the low amplitude Love wave predicted for INCN from the 2007 test INCN is near a Love wave node, and the location of the node is well constrained by other data. It may be that there is enough off azimuth Love wave energy to increase the amplitude significantly.

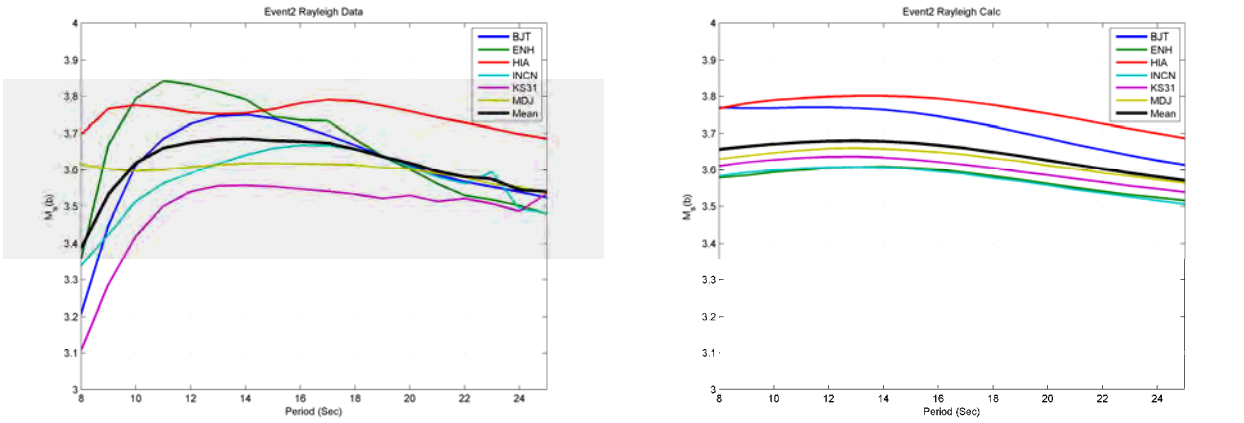

Figure 32. Rayleigh wave data from North Korea event #2 (left), and predicted data from moment tensor inversion (right).

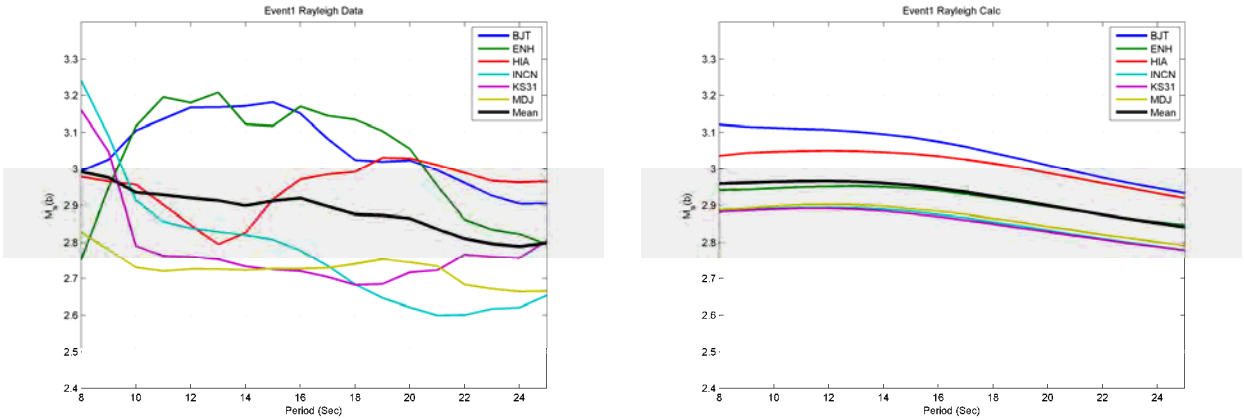

Figure 33. Rayleigh wave data from North Korea event #1 (left), and predicted data from moment tensor inversion (right).

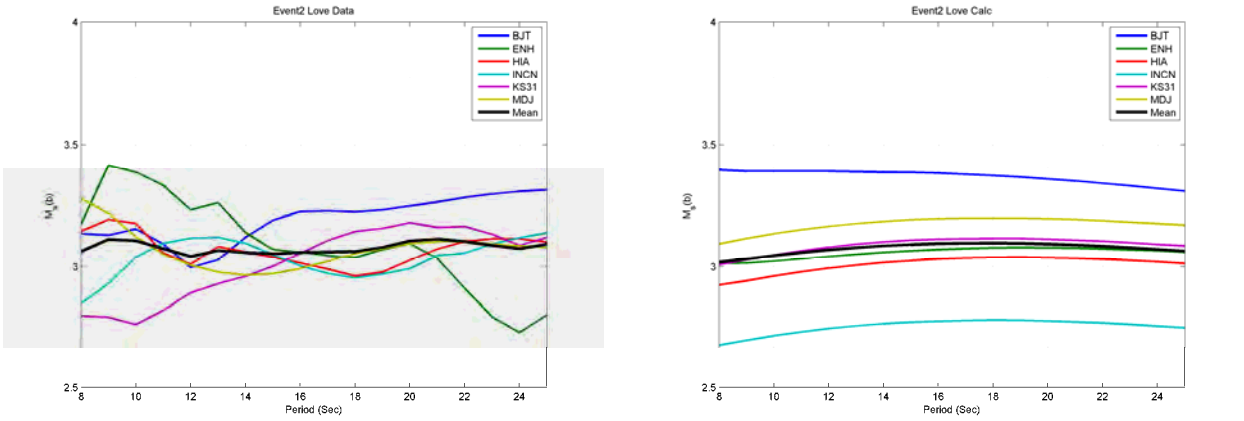

Figure 34. Love wave data from North Korea event #2 (left), and predicted data from moment tensor inversion (right).

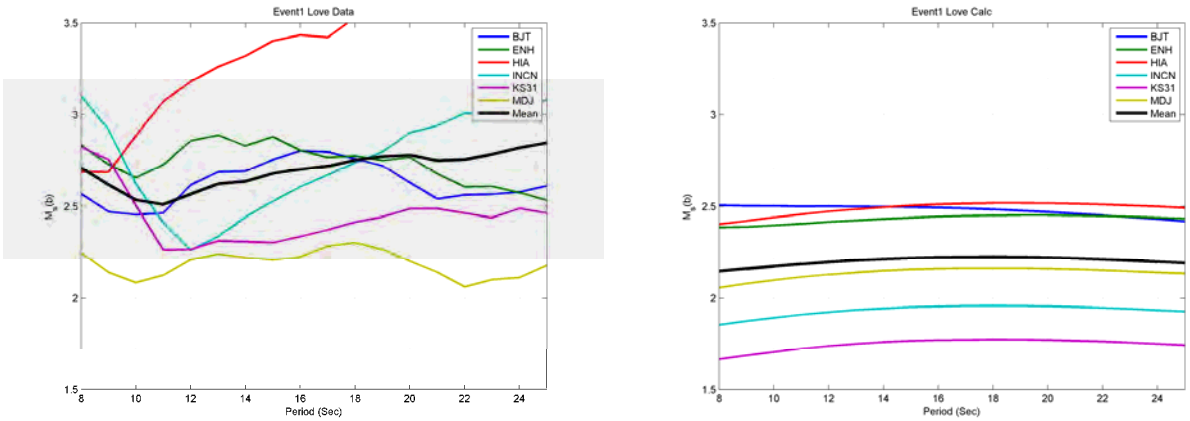

Figure 35. Love wave measurements from North Korea event #1 (left), and predicted data from moment tensor inversion (right). The measurements were made in the time window where a Love wave was expected; however, Love waves were close to or below the noise level so the data should be regarded as an upper bound on Love wave amplitudes.

The effects on the individual station M_s values predicted by the tectonic release moment tensor solution for the 2009 test are listed in Table 12. The net effect is predicted to increase the network-averaged M_s value by only 0.06 magnitude units, which is much too small to explain the observed anomaly. However, it should be noted that since the CLVD component does not generate Love waves, it is not well constrained in the inversion; and a larger CLVD component would generate larger M_s. That is, an explosion with the same isotropic moment and a larger CLVD would generate larger surface waves with the same Love waves, no additional Rayleigh wave azimuthal variation and only a small change in spectral shape. This possibility will need to be systematically evaluated in any future studies of the observed M_s anomalies.

Table 12. Change in M_s for Event 2 caused by tectonic release

Station	ΔMs
BJT	0.11
ENH	0.02
HIA	0.17
INCN	-0.01
KS31	0.02
MDJ	0.04
Average± Standard Deviation	0.06 ±0.07

In summary, the M_s values observed for the North Korean explosions were much higher than expected based on past experience with explosions at other test sites. The inferred non-isotropic contributions to the long-period sources for the NK explosions relative to Semipalatinsk are of opposite sign, and account for part of this difference. Uncertainties in the extrapolation from the experimental database of mostly larger explosions in lower velocity media may also contribute to the apparent anomaly. Nevertheless, it is not clear that there is any plausible combination of these two factors that is adequate to explain the observed offsets. Additional research will be required to more fully investigate possible sources of these observed M_s anomalies for the two North Korean nuclear tests.

4 Discrimination

4.1 Ms:mb Discriminant

The anomalously high Ms estimates for both the 2006 and 2009 events produced seemingly unrealistically high yield estimates. Further they severely impacted the Ms:mb discriminant, placing the events at or near the earthquake/explosion decision line. These results are discussed in the full contents of surface wave detection, yield estimation and moment tensor analysis discussed earlier. The reader is referred to Section 3.4 of this report starting on page 32.

4.2 High Frequency Pn/Lg Discriminant

While the Ms-vs-mb discriminant produces inconclusive screening results, identification of both events as explosions based on observed high-frequency Pn/Lg ratios at regional stations is unambiguous. In general, our results and analyses for Pn/Lg ratios corroborate the results of other authors (e.g. Walter et al., 1995; Kim and Richards, 2007; Kim et al., 2009; Fisk et al., 2009) which indicate large Pn/Lg ratios at high frequencies for nuclear explosions (and the North Korean explosions in particular) compared to other sources.

Prior to the North Korean nuclear tests, SAIC conducted a study to assess monitoring capabilities for North Korea (Kohl et al., 2004). As part of that, we carefully analyzed and calibrated procedures for determining Pn/Lg ratios from observations of seismic signals at regional stations for events in the region. Those analyses were based on approximately 400 events (including earthquakes and presumed mining blasts) from the Korean peninsula recorded at regional distances with stations mainly in South Korea and China. The observed Pn/Lg ratios in several frequency bands were used to calibrate and develop distance corrections for the various regional stations, which were then applied to normalize the observed ratios. These prior calibration studies showed that three-component (3-C) Pn/Lg ratios developed from higher-frequency passbands (in particular 7-9 Hz) and corrected for distance provided a clear distinction between explosions and earthquakes.

For this project we applied the same measurement techniques to the signals recorded at 11 regional stations for the 2009 North Korea nuclear explosion (Figure 36). As can be seen in the figure, the paths to the regional stations include a variety of propagation environments. In particular, it is well-known that oceanic path segments block Lg propagation; so regional Japanese stations (MAJO, JNU) do not see Lg for the NK explosion, although they do record good regional P (Pn). Furthermore, records at several of the more distant stations (e.g. BJT, HIA, ULN, ENH) appear to have some indication of Lg in broadband and at lower frequencies; but higher frequency Lg signals, which produce more effective source screening, are more severely attenuated over the long paths due to increased attenuation, falling to noise, and cannot be used. In the following analyses, we used only observations from regional stations for which both the Pn and Lg signals in the 7-9 Hz passband had Signal-to-Noise ratios (SNRs) of 2.0 or larger.

Figure 36. Regional stations considered for the Pn/Lg spectral ratio discriminant. Four of the stations had sufficient SNR for both Pn and Lg phases in the 7-9 Hz band.

For the 2009 North Korean nuclear test, we are left with signals with high SNRs in the 7-9 Hz passband for both Pn and Lg at four stations (MDJ, USRK, KSRS, and TJN) at distances from 3.3° to 5.1°. Although INCN is within the near-regional distance range, station noise levels are high (apparently due to local site conditions) and 7-9 Hz SNRs there are low (<2.0) for Pn and Lg phases for both the 2009 and 2006 events. It should be noted that the number of regional stations with useful SNRs represents an improvement over prior results (e.g. Bennett et al., 2006) which only showed observations from two stations (MDJ and KSRS) for the 2006 North Korean explosion. The corresponding 7-9 Hz Pn/Lg ratios at the individual stations are plotted in Figure 37, along with similar observations for sample events including earthquakes and mine blasts on the Korean peninsula from our prior calibration study (Kohl et al., 2004) and from the same stations for the 2006 North Korean nuclear test (Bennett et al., 2006). Note that for station USRK 3-C data were not available for the 2009 event, so we used the vertical component Pn/Lg ratio as a surrogate in these plots; and USRK was not available at all for the 2006 event. The plot in Figure 37 also shows the distance correction used to normalize the individual station measurements preliminary to network averaging. The Pn/Lg ratio station observations for both the 2009 and 2006 NK nuclear tests in Figure 37 are clearly significantly larger than similar ratios for earthquakes and tend to match observations from mining explosions with the distance correction applied (based on the historical calibration data from the Korean peninsula noted above).

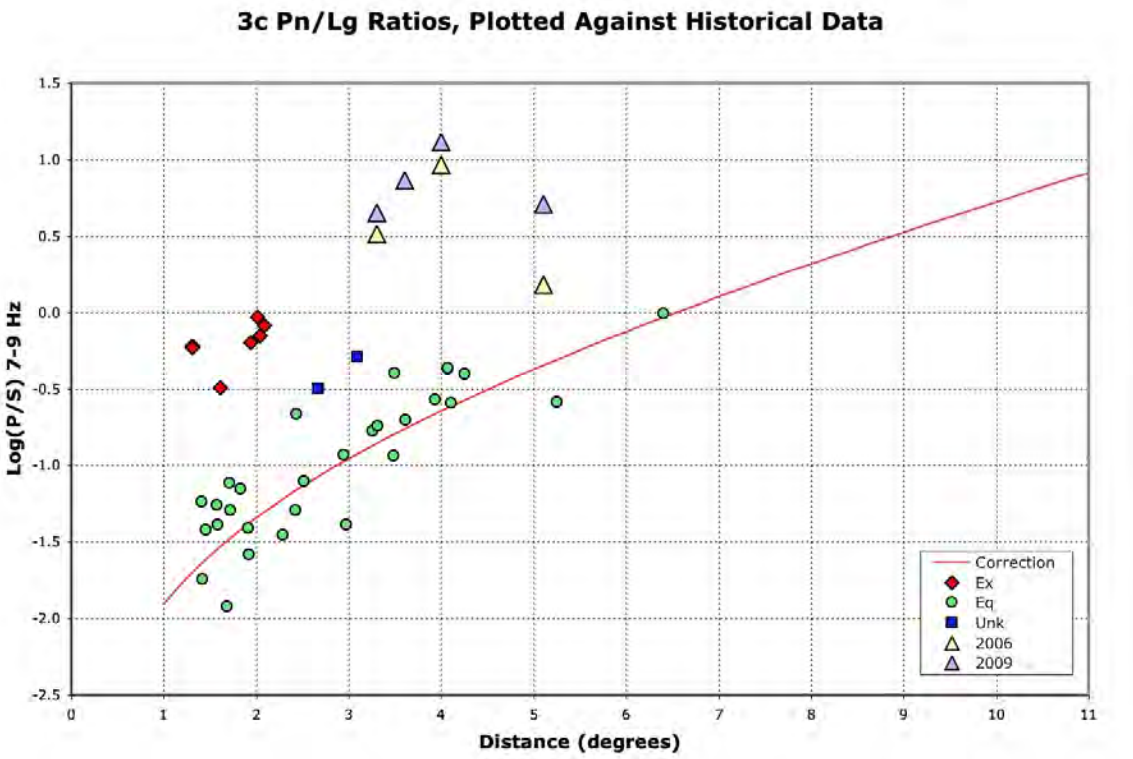

Figure 37. High-frequency Pn/Lg ratio measurements (KSRS, MDJ, TJN, USRK) plotted against selected historical data. The red curve shows the distance correction function derived by Kohl et al. (2004) for continental paths to events on the Korean Peninsula.

Figure 38 shows the distance-normalized and network-averaged 7-9 Hz Pn/Lg ratios for the 2009 North Korean nuclear test, along with similar measurements from the Korean peninsula developed during the North Korea calibration study (Kohl et al., 2004) and for the post-event analyses of the 2006 nuclear test (Bennett et al., 2006). The 2009 result shows a very large Pn/Lg ratio metric, at the upper bounds of the range from commercial explosions and clearly distinct from earthquakes in the same region. While the 2006 event is consistent with the hypothesis of an explosion source (i.e. the 95% confidence bound overlaps the commercial explosion sample), the 2009 event actually lies well above most explosions and the 95% confidence bounds do not overlap the explosion decision line (red dashed). The latter observation is potentially due to the fact that the known explosions from the Korean peninsula (red diamonds) were all chemical (e.g. mine blasts) with a less impulsive source than what might be expected from a nuclear explosion.

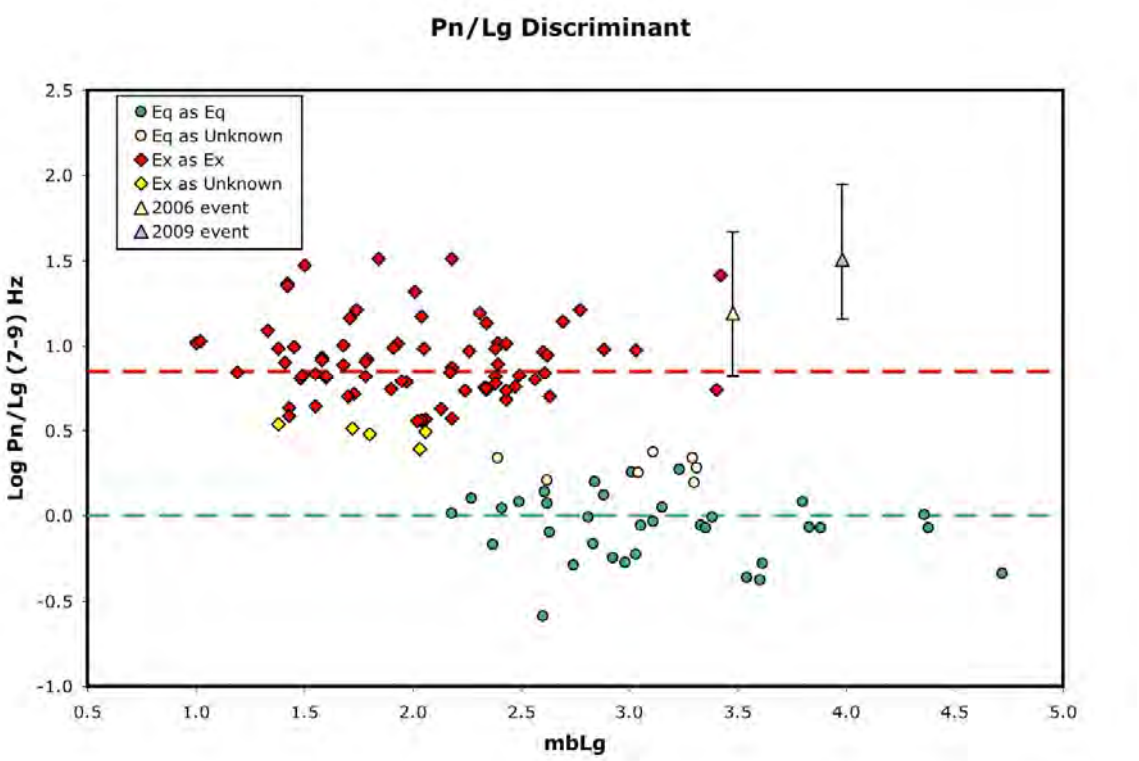

Figure 38. Pn/Lg discriminant test for the 2006 and 2009 North Korean tests plotted against historical data. The distance corrected, station averaged spectral ratios are shown along with the 95% confidence interval.

5 Conclusions

On May 25, 2009 the North Koreans conducted a second underground nuclear test at a location very close to that of their initial 2006 test in a remote, mountainous region of northeastern North Korea. The objective of the present study has been to exploit IMS and other open data sources to conduct comprehensive, advanced analyses of the characteristics of these two North Korean nuclear tests. These studies focused on refining event locations, estimating source depths and seismic yields and evaluating the effectiveness of the various seismic event identification criteria as applied to these two explosions. Seismic data recorded at stations of the global IMS network were augmented with seismic data from key regional stations (Δ<20degrees) obtained from the Incorporated Research Institutions for Seismology (IRIS) data management center, the Ocean Hemisphere Project Data Management Center (OPHDMC) and the Japanese National Research Institute for Earth Science and Disaster Prevention (NIED). The principal findings of these analyses with regard to the characterization of the North Korean nuclear tests can be summarized as follows:

- Available seismic arrival time data from the 2006 and 2009 tests were analyzed using a variety of state-of-the-art relative location techniques. All of the resulting solutions yielded very similar locations, indicating that the 2009 test was conducted about 2.5 km west-northwest of the 2006 test. Supplemental topographic data for the site were used to further constrain the absolute locations with respect to the tunnel adit entry identified from open source overhead imagery.
- Teleseismic P wave spectral data were inverted using a model-based procedure to determine the yield of the 2009 test. Because source depth is poorly constrained using conventional seismic techniques, yield estimates were determined at 100 m increments over the plausible depth range from 100 to 800 m. These yield estimates vary from 2.0 to 4.8 kt.
- Since the uncertainty in source depth leads to considerable uncertainty in the yield estimate, a new technique based on broadband source spectral ratios was developed to better constrain the depths of the 2006 and 2009 explosions. The results of this analysis indicate that the two explosions could not have been conducted at any common depth in the plausible 100 to 800 m range; and, in fact, the observed spectral ratio data are best modeled by source depths of about 200 m for the 2006 test and 550 m for the 2009 test. The corresponding yield estimates for the 2006 and 2009 tests are 0.9 kt and 4.6 kt., respectively.
- Relative yield estimates based on Lg observations from the two tests are generally consistent with the yield estimates obtained by modeling the network-averaged teleseismic P wave spectra and the estimates obtained by modeling the regional, broadband P wave source spectral ratios.
- The long-period surface wave Ms magnitudes for both the 2006 and 2009 tests appear to be anomalously large relative to historical experience, producing unreasonably large Ms yield estimates and problematic Ms/mb identification characteristics. A formal moment tensor inversion analysis of the available data has indicated that release of tectonic strain energy by the explosion may have contributed somewhat to the observed anomaly. However, current estimates of the likely strength of this tectonic release are not large

enough to fully explain the observed anomaly. Additional research will be required to determine whether unresolved CLVD secondary sources any account for the discrepancy.

- Identification of the 2009 and 2006 events as explosions based on high-frequency Pn/Lg ratios measured at regional stations are unambiguous; however, results for discrimination based on Ms-versus-mb are inconclusive (again probably due to secondary source contamination to Ms).

6 References

Bennett J, North B, Kohl B, Murphy J, Stevens J, Bondar I, Fisk M, Bahavar M, Barker B, Israelsson H and V Oancea, 2006, Analysis of IMS data from the North Korean (DPRK) Nuclear Test of October 9, 2006, SAIC, SAIC Technical Report SAIC-06/2203.

Bonner, Jessie, Robert B. Herrmann, David Harkrider, and Michael Pasyanos (2008), The Surface Wave Magnitude for the 9 October 2006 North Korean Nuclear Explosion, Bulletin of the Seismological Society of America, Vol. 98, No. 5, pp. 2498–2506, October 2008, doi: 10.1785/0120080929.

Che, Il-Young, Tae Sung Kim, Jeong-Soo Jeon and Hee-Il Lee (2009) Infrasound observation of the apparent North Korean nuclear test of 25 May 2009, Geophysical Research Letters, Vol. 36, L22802, doi:10.1029/2009GL041017.

Cho, M. (2008). Tectonomorphic Evolution of Collisional Orogenic Belts in the Korean Peninsula: Implications for East Asian Tectonics, Himalayan Journal of Sciences, 5, p. 40.

Chun, Kin-Yip, and Gary A. Henderson (2009), Lg Attenuation near the North Korean Border with China, Part II: Model Development from the 2006 Nuclear Explosion in North Korea, Bulletin of the Seismological Society of America, Vol. 99, No. 5, pp. 3030–3038, October 2009, doi: 10.1785/0120080341.

Chun, Kin-Yip, Yan Wu, and Gary A. Henderson (2009), Lg Attenuation near the North Korean Border with China, Part I: Model Development from Regional Earthquake Sources, Bulletin of the Seismological Society of America, Vol. 99, No. 5, pp. 3021–3029, October 2009, doi: 10.1785/0120080316.

Day, S. M., and J. L. Stevens (1986), "An explanation for apparent time delays in phase-reversed Rayleigh waves from underground nuclear explosions," Geophysical Research Letters, v. 13, pp. 1423-1425.

Dewey, J. W., 1972, Seismicity and Tectonics of Western Venezuela, Bulletin of the Seismological Society of America. VoL 62, No. 6, pp. 1711-1751. December 1972.

Fisk, M. D., 2002, Accurate Locations of Nuclear Explosions at the Lop Nor Test Site Using Alignment of Seismograms and IKONOS Satellite Imagery Bulletin of the Seismological Society of America, Vol. 92, No. 8, pp. 2911–2925, December 2002.

Fisk, Mark D., Steven R. Taylor, William R. Walter, and George E. Randall (2009), Seismic Event Discrimination Using Two-Dimensional Grids Of Regional P/S Spectral Ratios: Applications To Novaya Zemlya And The Korean Peninsula, 2009 Monitoring Research Review: Ground-Based Nuclear Explosion Monitoring Technologies.

Ford, Sean R., Douglas S. Dreger, and William R. Walter (2009), Source analysis of the Memorial Day explosion, Kimchaek, North Korea, Geophysical Research Letters, Vol. 36, L21304, doi:10.1029/2009GL040003.

Given, J. W. and G. R. Mellman (1986), “Estimating Explosion and Tectonic Release Source Parameters of Underground Nuclear Explosions from Rayleigh and Love wave Observations,” Sierra Geophysics Final Report to Air Force Geophysics Laboratory, Part 1, AFGL-TR-86-0171, SGI-R-86-126, July.

GlobalSecurity.org (2006). Weapons of Mass Destruction (WMD): Possible North Korean Nuclear Test Site near Punggye-yok, online at http://www.globalsecurity.org/wmd/world/dprk/kilju-punggye-yok.html.

Grubbs, F E, 1950, Sample Criteria for testing outlying observations. Ann. Math. Stat. 21, 1, 27-58.

Herrmann, R., V. Hsu, and L. Malagnini (1996). Attenuation Studies for the Korea Region, Proc. of the February 1996 Workshop on Seismic Location and Discrimination in Korea, Phillips Lab Report PL-TR-96-2086, 313-322.

Herrmann, R., Y. Jeon, H. Yoo, K. Cho, W. Walter, M. Pasyanos (2006). Seismic Source and Path Calibration in the Korean Peninsula, Yellow Sea, and Northeast China, Proc. 28th Seismic Research Review: Ground-Based Nuclear Explosion Monitoring Technologies, 60-70.

Hong Tae-Kyung, and Junkee Rhie (2009), Regional Source Scaling of the 9 October 2006 Underground Nuclear Explosion in North Korea, Bulletin of the Seismological Society of America, Vol. 99, No. 4, pp. 2523–2540, August 2009, doi: 10.1785/0120080007.

Hong, Tae-Kyung, Chang-Eob Baag, Hoseon Choi, and Dong-Hoon Sheen (2008), Regional seismic observations of the 9 October 2006 underground nuclear explosion in North Korea and the influence of crustal structure on regional phases, Journal Of Geophysical Research, Vol. 113, B03305, doi:10.1029/2007JB004950.

Kim W.-Y., and P. G. Richards (2007), North Korean Nuclear Test: Seismic Discrimination at Low Yield, Eos, Vol. 88, No. 14, 3 April 2007.

Kim, Tae Sung, Ik-Bum Kang, and Geun-Young Kim (2009), Yield ratio estimates using regional Pn and Pg from North Korea's underground nuclear explosions, Geophysical Research Letters, Vol. 36, L22302, doi:10.1029/2009GL040495, 2009.

Kohl, B., B. Barker, J. Bennett, I. Bondar, M. Fisk, H. Israelsson, K. McLaughlin, W. Nagy, M. Skov, J. Stevens, X. Yang, and B. Zuzolo (2004), Application of Advanced Seismo-Acoustic Technologies to Regional Monitoring of North Korea, SAIC, SAIC Technical Report SAIC-04/2200.

Koper, Keith D., Robert B. Herrmann, Harley M. Benz (2007), Overview of Open seismic data from the north korean event of 9 October 2006, Seismological Research Letters Volume 79, Number 2 March/April 2008 doi: 10.1785/gssrl.79.2.178.

Kværna, Tormod, Frode Ringdal, and Ulf Baadshaug (2007), North Korea's Nuclear Test: The Capability for Seismic Monitoring of the North Korean Test Site, Seismological Research Letters Volume 78, Number 5 September/October 2007.

Lambert, D. and S. Alexander (1971), "Relationship of body and surface wave magnitudes for small earthquakes and explosions," Teledyne Geotech Seismic Data Laboratory report number 245 to Air Force Technical Applications Center.

Mueller, R. A. and J. R. Murphy (1971), "Seismic characterization of underground nuclear detonations. Part 1: Seismic scaling law of underground nuclear detonations," *Bull. Seism. Soc. Am.*, **61**, 1675-1692.

Murphy, J. R. (1977), "Seismic Source Functions and Magnitude Determinations for Underground Nuclear Detonations," *Bull. Seism. Soc. Am.*, **67**, 135-158.

Murphy, J. R. (1995), "Types of seismic events and their source descriptions," in Monitoring a Comprehensive Test Ban Treaty, ed. E. Husebye and A. Dainty, pp. 225–245, Kluwer Academic Publishers, Boston.

Nuttli, O. (1986a), "Yield estimates of Nevada test site explosions obtained from seismic Lg waves," *J. Geophys. Res*., 91, 2137-2151.

Nuttli, O. (1986b), "Lg magnitudes of selected East Kazakhstan underground explosions," *Bull. Seism. Soc. Am.*, 76, 1241-1251.

Patton, H. (1988), "Application of Nuttli's method to estimate the yield of the Nevada test site explosions recorded by the Lawrence Livermore National Laboratory's seismic system," *Bull. Seism. Soc. Am.*, 78, 1759-1772.

Patton, Howard J. and Steven R. Taylor (2008), Effects of shock-induced tensile failure on mb-Ms discrimination: Contrasts between historic nuclear explosions and the North Korean test of 9 October 2006, Geophysical Research Letters, Vol. 35, L14301, doi:10.1029/2008GL034211.

Priestley, K., and H. Patton (1997), "Calibration of mb(Pn), mb(Lg) scales and transportability of the M0:mb discriminant to new tectonic regions," Bull. Seism. Soc. Am., 87, 1083-1099.

Richards, Paul G. and Won-Young Kim (2007), Seismic signature, nature physics | Vol 3 | January 2007.

Russell, D. R. (2006), "Development of a time-domain, variable period surface-wave magnitude measurement procedure for application at regional and teleseismic distances, part I: theory," *Bull. Seism. Soc. Am.*, **96**, 665-677, doi: 10.1785/0120050055.

Salzberg, David H., Semi-Empirical Yield Estimates For The 2006 North Korean Explosion, 2008 Monitoring Research Review: Ground-Based Nuclear Explosion Monitoring Technologies.

Schlittenhadt, J., M. Canty, and I. Gruenberg (2010). Satellite Earth Observations Support CTBT Monitoring: Case Studies Including the Nuclear Test in North Korea of Oct. 9, 2006 and Comparison with Seismic Results, *Pure and Applied Geophysics*, 10.1007/s00024-009-0036-x, 22 January 2010.

Selby, N. (2007). "Implications of the 9 October 2006 North Korean nuclear test for event screening" (abstract), *Seism. Res. Lett.*, **78**, 253.

Selby, N.D, D Bowers (2009), Preliminary Seismological Investigation by the UK NDC of the announced DPRK Nuclear Test of 25th May 2009, AWE Technical Report, July 2009.

Shin, Jin Soo, Dong-Hoon Sheen and Geunyoung Kim (2009), Regional observations of the second North Korean nuclear test on 2009 May 25, Geophys. J. Int. (2010) 180, 243–250 doi: 10.1111/j.1365-246X.2009.04422.x.

Snieder, R., and M. Vrijlandt (2005), Constraining the source separation with coda wave interferometry: Theory and application to earthquake doubles in the Hayward fault, California, *J. Geophys. Res*. **10** (B04301), DOI:10.1029/2004JB003317.

Stevens, J. L. (1982), "A model for tectonic strain release from explosions in complex prestress fields applied to seismic waves from NTS and Eastern Kazakh explosions," Systems, Science and Software technical report submitted to VELA Seismological Center, SSS-R-82-5358, January.

Stevens, J. L. and J. R. Murphy (2001), "Yield Estimation from surface wave amplitudes," *Pure and Applied Geophysics*, **158**, 2227-2251.

Stevens, J. L. and S. M. Day (1985), "The physical basis of the mb:Ms and variable frequency magnitude methods for earthquake/explosion discrimination," Journal of Geophysical Research, **90**, 3009-3020.

Stevens, J. L., G. E. Baker and H. Xu (2007), "The Physical Basis of the Explosion Source and Generation of Regional Seismic Phases," SAIC final report submitted to Air Force Research Laboratory, September.

Stevens, Jeffry L., Jeffrey W. Given, Heming Xu, and G. Eli Baker (2007), "Development of Surface Wave Dispersion and Attenuation Maps and Improved Methods for Measuring Surface Waves," Proceedings of the 29thAnnual Monitoring Research Review, Denver, CO, 25-27 September 2007.

Sultanov, D. D., J. R. Murphy and K. D. Rubinstein (1999), "A seismic source summary of Soviet peaceful nuclear explosions," *Bull. Seism. Soc. Am.*, **89**, 640-647.

Tibuleac, Ileana M., David H. von Seggern, John G. Anderson, Kenneth W. Smith, Arturo Aburto, and Thomas Rennie (2008), Location and Magnitude Estimation of the 9 October 2006 Korean Nuclear Explosion Using the Southern Great Basin Digital Seismic Network as a Large-Aperture Array, Bulletin of the Seismological Society of America, Vol. 98, No. 2, pp. 756–767, April 2008, doi: 10.1785/0120070046.

US Geological Survey (1966-1969). Military Geology Branch Atlases of Asia and Eastern Europe to Support Detection of Underground Nuclear Testing, prepared for DARPA.

USGS/NEIC (2010). Magnitude Definitions Used by the NEIC, http://neic.usgs.gov/neis/phase_data/mag_formulas.html .

Waldhauser F and W L Ellsworth, (2000), A Double-Difference Earthquake Location Algorithm: Method and Application to the Northern Hayward Fault, California, Bulletin of the Seismological Society of America, 90, 6, pp. 1353–1368, December 2000.

Waldhauser F, Schaff D, Richards P G, and Won-Young Kim, (2004), Lop Nor Revisited: Underground Nuclear Explosion Locations, 1976–1996, from Double-Difference Analysis of Regional and Teleseismic Data Bulletin of the Seismological Society of America, Vol. 94, No. 5, pp. 1879–1889, October 2004.

Walter, W. R., Fisk, M. D. and Taylor, S. R. (2007), A Review Of Empirical Observations Of Earthquake-Explosion Discrimination Using P/S Ratios And Implications For The Sources Of Explosion S-Waves, Proceedings of the 2007 SSA Meeting.

Zhao, Lian-Feng, Xiao-Bi Xie, Wei-Min Wang, and Zhen-Xing Yao (2008), Regional Seismic Characteristics of the 9 October 2006 North Korean Nuclear Test, Bulletin of the Seismological Society of America, Vol. 98, No. 6, pp. 2571–2589, December 2008, doi: 10.1785/0120080128.